



CZECH TECHNICAL UNIVERSITY IN PRAGUE
Faculty of Nuclear Sciences and Physical Engineering
Department of Physics



Two-particle quantum walk on percolated graph

Kvantová procházka dvou částic na perkolovaném grafu

Masters's Degree Project

Author: **Bc. Magdalena Parýzková**
Supervisor: **doc. Ing. Martin Štefaňák, Ph.D.**
Consultant: **Ing. Jaroslav Novotný, Ph.D.**
Academic year: 2022/2023



Katedra: fyziky

Akademický rok: 2021/2022

ZADÁNÍ DIPLOMOVÉ PRÁCE

Student: Bc. Magdalena Parýzková

Studijní program: Matematická fyzika

Název práce: Kvantová procházka dvou částic na perkolovaném grafu
(česky)

Název práce: Two-particle quantum walk on percolated graph
(anglicky)

Pokyny pro vypracování:

- 1) Kvantová procházka s mincí dimenze 2 pro jednu a dvě částice na přímce, kružnici a úsečce
- 2) Kvantová procházka jedné částice na dynamicky perkolovaných grafech, asymptotické chování, atraktorový prostor, p-atraktory
- 3) Kvantová procházka dvou částic na dynamicky perkolovaném grafu, úplnost nalezených řešení atraktorových rovnic, porovnání s výsledky pro jednu částici
- 4) Možná rozšíření např. pro procházku s mincí dimenze 3, vliv na kvantový transport

Doporučená literatura:

- [1] B. Kollár, T. Kiss, J. Novotný, I. Jex: Asymptotic Dynamics of Coined Quantum Walks on Percolation Graphs. Phys. Rev. Lett. 108, 230505 (2012)
- [2] B. Kollár, J. Novotný, T. Kiss, I. Jex: Discrete time quantum walks on percolation graphs. Eur. Phys. J. Plus 129, 103 (2014)
- [3] B. Kollár, J. Novotný, T. Kiss, I. Jex: Percolation induced effects in two-dimensional coined quantum walks: analytic asymptotic solutions. New J. Phys. 16, 023002 (2014)
- [4] M. Štefaňák, J. Novotný, and I. Jex: Percolation assisted excitation transport in discrete-time quantum walks. New J. Phys. 18, 023040 (2016)
- [5] J. Mareš, J. Novotný, and I. Jex: Percolated quantum walks with a general shift operator: From trapping to transport. Phys. Rev. A 99, 042129 (2019)

Jméno a pracoviště vedoucího diplomové práce:

doc. Ing. Martin Štefaňák, Ph.D.

Katedra fyziky, Fakulta jaderná a fyzikálně inženýrská ČVUT v Praze

konzultant:

Ing. Jaroslav Novotný, Ph.D.

Katedra fyziky, Fakulta jaderná a fyzikálně inženýrská ČVUT v Praze

Datum zadání diplomové práce: 20.10.2021

Termín odevzdání diplomové práce: 02.05.2022

Doba platnosti zadání je dva roky od data zadání.



.....
garant studijního programu



.....
vedoucí katedry



.....
děkan

V Praze dne 20.10.2021



PROHLÁŠENÍ

Já, níže podepsaná

Jméno a příjmení studenta: Magdalena Parýzková

Osobní číslo: 476590

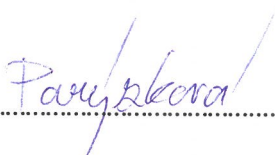
Název studijního programu (oboru): Matematická fyzika

prohlašuji, že jsem diplomovou práci s názvem:

Kvantová procházka dvou částic na perkolovaném grafu

vypracovala samostatně a uvedla veškeré použité informační zdroje v souladu s Metodickým pokynem o dodržování etických principů při přípravě vysokoškolských závěrečných prací.

V Praze dne 5.1.2023


.....

podpis

Acknowledgment:

I would like to thank my supervisor doc. Ing. Martin Štefaňák, Ph.D. for his time, help and kindness. Furthermore, I would like to thank my family and friends for their endless support and patience.

Název práce:

Kvantová procházka dvou částic na perkolovaném grafu

Autor: Bc. Magdalena Parýzková

Studijní program: Matematická fyzika

Druh práce: Diplomová práce

Vedoucí práce: doc. Ing. Martin Štefaňák, PhD., Katedra fyziky, Fakulta jaderná a fyzikálně inženýrská ČVUT v Praze

Konzultant: Ing. Jaroslav Novotný, PhD., Katedra fyziky, Fakulta jaderná a fyzikálně inženýrská ČVUT v Praze

Abstrakt: Dynamicky perkolované grafy jsou grafy s hranami, které se mohou náhodně lámat v každém kroku kvantové procházky. Ačkoliv mohou dynamické perkolace simulovat systémy s možnými nedokonalostmi, jsou stále obecně poměrně složité pro analýzu. Existuje nicméně zavedený formalismus, který umožňuje studium jejich asymptotického vývoje. S jeho pomocí už byly v minulosti nalezeny zajímavé vlastnosti právě perkolovaných jednočásticových kvantových procházek v diskrétním čase. Například fakt, že možnost náhodného lámání hran může zlepšit transportní vlastnosti systému. Vzhledem k tomu, že vícečásticové kvantové procházky jsou známé svými zajímavými vlastnostmi a možnými aplikacemi, zabývá se tato práce právě případem dvoučásticových kvantových procházek v diskrétní čase v jedné dimenzi. Konkrétně pak studuje řešení asymptotického vývoje pro speciální případ Hadamardovy procházky na úsečce a na kružnici.

Klíčová slova: atraktory, asymptotický vývoj, kvantové procházky v diskrétním čase, dvě částice, perkolace

Title: **Two-particle quantum walk on percolated graph**

Author: Bc. Magdalena Parýzková

Abstract: Dynamically percolated graphs are graphs with edges which can get randomly broken at every time step of the quantum walk. While dynamical percolations can simulate systems with possible imperfections, they are still generally difficult to study. However, there is an existing formalism that allows us to analytically investigate the asymptotic evolution of such systems. This has already revealed some of the interesting properties of the discrete-time percolated single-particle quantum walks. Namely, for some graphs, the possibility of broken edges causes an improvement in the system's transport properties. As multi-particle quantum walks are generally known for their interesting properties and possible applications, this thesis focuses mainly on the two-particle discrete-time quantum walks in one dimension. Specifically, it studies the asymptotic evolution of the dynamically percolated two-particle Hadamard walk on a finite line and a circle.

Key words: attractors, asymptotic evolution, discrete time quantum walks, percolations, two particles

Contents

Introduction	11
1 One-particle quantum walks	13
1.1 Quantum walks in one dimension	15
1.2 Coin operator and equivalence classes	17
1.3 Solution using Fourier transform	19
2 Asymptotic evolution and percolated quantum walks	23
2.1 Asymptotic evolution	24
2.2 Hadamard walk on a finite line and a circle	29
2.3 Lazy walk	32
3 Two-particle quantum walks	35
3.1 Introducing interaction	40
3.2 Percolated quantum walks	42
4 Asymptotic evolution of percolated two-particle walk	45
4.1 Shift conditions	45
4.1.1 Boundary conditions	47
4.2 Coin condition	47
4.3 Finding p-attractors	48
4.3.1 Circle	51
4.4 Non-p-attractors	51
4.4.1 Circle	53
4.4.2 Summary and orthonormal basis	53
4.5 Proof of completeness	55
4.6 Indistinguishable particles	59
4.7 Asymptotic state for circles of lengths $N \neq 4k$	61
4.8 Mapping to one-particle walk	63
4.9 Possible extensions	63
Conclusion	65

Introduction

Quantum random walks have been studied as a quantum equivalent of the classical random walks since the first introduction of the term in 1993 [1]. However, the first idea of quantum walks, although in quite different form than they are known today, originated from Richard Feynman in 1940s. In the classical realm random walks are one of the basic objects of study in probability theory and their applications have been found in many different fields including physics, chemistry, biology, financial economics, etc.. They can be defined in both discrete and continuous time and space and the limit transitions between those are quite well understood. Probably the most well known examples are the drunken sailor and the Brownian motion. The drunken sailor describes the simplest random walk on a line in discrete time and space. Basically the sailor starts in a pub and in every time step he makes one step either right, or left, both with fifty percent probability. The question is then, how will the probability distribution of the sailor's position look like in time. It turns out, that in this case one will get a binomial distribution centered in the pub, i.e. the origin of the walk. The example of Brownian motion can then, in a very simplified and shortened version, be understood as just a generalization to two-dimensional continuous space.

As for the quantum equivalent of random walks, it has found its use in several fields as well including biology, chemistry and quantum computing and information. Probably their most famous application is in the realm of quantum search algorithms in both their discrete-time and continuous-time version. It turns out that by organizing an unordered database into a certain graph structure, quantum walk can also provide a quadratic speed up as is typical for quantum search algorithms in general. Interestingly it has been proved that almost all graphs provide this quadratic speed-up [2]. Another often studied positive effects lie in the transport of excitation through some graph represented systems. As for quantum computing in general, quantum walks were also shown to be capable of universal quantum computing in both the discrete-time and the continuous-time version. The schemes for building the quantum gates are so far quite complicated, however, they do prove the computational power of the quantum walks. The first to show this was the work of A. Childs from 2009 [3] where the universal computation via quantum walks was shown for the continuous-time quantum walk. Later also came a version using multi-particle continuous-time quantum walks [4] from the same author. As for the discrete-time walks, the scheme for the construction of quantum circuits was published in 2010 by N. B. Lovett et al. in [5]. And recently another version using discrete-time quantum walks appeared also in [6].

Quantum walks on percolated graphs, where the edges of the graph can disappear and reappear again randomly in every step of the walk, have been studied previously for both the discrete time and the continuous time quantum walks. For the single-walker discrete-time walks these kinds of environments seem to help with transport of quantum excitation as has been showed previously e.g. in [7], [8] or [9]. Although studying these systems usually becomes more difficult due to the additional randomness introduced, in the asymptotic limit of large time the evolution can actually be obtained analytically [10].

In this work the case of two-walker discrete-time percolated quantum walks in one dimension will be studied, more specifically, the asymptotic evolution of this system on a finite line and a circle. The first

chapter provides a short introduction on the one-particle discrete-time quantum walks in general and then discusses in more detail the case of the walk on a line. The second chapter then discusses the formalism and methods necessary for studying the asymptotic evolution of quantum walks on percolated graphs. In the third chapter the two-particle quantum walks will be discussed together with the previous works on both the non-percolated and the percolated two-particle walks. The last chapter will finally show the found solutions for the asymptotic evolution of two-walker discrete-time percolated quantum walks in one dimension. Namely, the special case of the Hadamard walk on finite line and circle of different lengths.

Chapter 1

One-particle quantum walks

This first introductory chapter will consist of an explanation of the term discrete-time quantum walks and the formalism connected to them. It will especially focus on the definitions and known results of one-particle walks in one dimension, i.e. infinite line, finite line and circle.

Generally, the classical random walks are defined as Markov chains of positions of the walker. Very simply speaking only the previous position distribution has some influence on the next one. In case of a discrete space of size N the probability distribution in a given time $t \in \mathbb{N}$ can be described by a vector $p(t) \in \mathbb{R}^N$. The vector consists of the probabilities of the walker being on individual positions. The evolution is then described by a stochastic matrix $M \in \mathbb{R}^{N,N}$ applied to the vector

$$p(t+1) = Mp(t). \quad (1.1)$$

As for the continuous time, by defining classical lazy walk, where the walker has some small probability of moving to the next site ϵ and also the probability of staying in place $1 - \epsilon$, and then making the limit $\epsilon \rightarrow 0$ one can eventually obtain the evolution of a continuous Markov chain given as

$$\frac{dp(t)}{dt} = Lp(t), \quad (1.2)$$

where $L = M - I$ and $p(t)$ still represents the probabilities. This is an example of how the continuous limits usually work quite nicely in the classical realm. However, the quantum equivalent of random walks can be much more challenging in that regard because of the coin space present in the discrete time variant [11–14]. It is important to note that this was just a very general introduction to a very vast and complex field on its own. The aim was just to give the reader an idea about what are the quantum walks actually a quantum equivalent to.

As for the actual definition of the discrete-time quantum walk on some general graph $G(V, E)$, where V denotes the set of vertices and E the set of edges, let's start with the Hilbert space of this quantum system. The first necessary thing is to define the position space of the walker spanned by basis states representing the vertices

$$\mathcal{H}_p = \{|v\rangle | v \in V\}. \quad (1.3)$$

However, this space needs to be augmented by coin degrees of freedom which represent the outgoing edges on a given vertex. More specifically vertex subspaces are defined as

$$\mathcal{H}_v = \{|v\rangle \otimes |c\rangle | c \in \{1, \dots, d_v\}\}, \quad (1.4)$$

where d_v is the degree of the vertex $v \in V$. The vectors $|c\rangle$ in the tensor product are possible states of the coin in the given subspace. They represent the direction of the walker, i.e. on which outgoing edge it

will walk in the next step. The whole Hilbert state of the quantum walk is then defined as a direct sum of these vertex subspaces

$$\mathcal{H} = \bigoplus_{v \in V} \mathcal{H}_v. \quad (1.5)$$

For d -regular graphs, i.e. graphs where all of the vertices are of the same degree d , this definition is equivalent to

$$\mathcal{H} = \mathcal{H}_p \otimes \mathcal{H}_c, \quad (1.6)$$

where \mathcal{H}_c is called a coin space

$$\mathcal{H}_c = \{|c\rangle \mid c \in \{1, \dots, d\}\}. \quad (1.7)$$

Since most of the work done in the literature is for d -regular graphs, the second definition (1.6) is more common. However, clearly it is not suitable for non-regular graphs, which is why (1.5) is more general. In both cases the basis states of the Hilbert space are in the form of a tensor product of the position and coin states. The following notation for these basis states will be used from now on

$$|v\rangle \otimes |c\rangle \equiv |v, c\rangle. \quad (1.8)$$

Moving on to the evolution of the system, the evolution operator is defined as a unitary operator on \mathcal{H} of the form

$$U = SC, \quad (1.9)$$

where S is called the **shift operator** and C called the **coin operator**. the coin operator basically represents the 'coin toss' of the quantum walker and is defined as an arbitrary unitary operator acting solely on the coin degrees of freedom. In the general case (1.5) it can be written down as

$$C = \bigoplus_{v \in V} C_v, \quad (1.10)$$

where C_v are local unitary coin operators for the given vertices. For the d -regular graphs with the same local coin operation C on every vertex the global coin operator can be equivalently written down simply as

$$C = I \otimes C. \quad (1.11)$$

The shift operator S is then a unitary operator which represents the jump of the walker to the next vertex according to the current state of the coin. There are again numerous ways how exactly the shift operator can be defined. One of the most general examples is the **flip-flop shift operator** defined in the following way. The walker jumps from the original vertex to the next one according to the coin state and then turns around. This can be written down as

$$S^{FL} = \sum_{v_1, v_2 \in V} |v_2, c(v_1)\rangle \langle v_1, c(v_2)|, \quad (1.12)$$

where $|c(v)\rangle$ denotes the coin state corresponding to the edge which leads to the vertex v . One can also add local permutations of the local coin states to the flip-flop operator in order to get a more general class of shift operators [7]. However, another shift operator will be used in this work, the **continuing shift operator**, which will be defined later for the case of one-dimensional walks. It works for example also for two-dimensional lattices where the difference between flip-flop and continuing shift operator can be seen quite clearly [15].

Each step of the walk the whole evolution operator is applied, so for the initial state $|\psi(0)\rangle \in \mathcal{H}$ of the walker the state after t steps will be

$$|\psi(t)\rangle = U^t |\psi(0)\rangle. \quad (1.13)$$

There is also an option to define the evolution operator in the opposite way as $U = CS$. The evolutions of both definitions will clearly be equivalent if the coin operator is applied on both the initial and final state. Since C is unitary, this only represents rotation to a different basis.

There exist of course even more complicated models of quantum walks, which will not be discussed here in detail. For example the evolution operator can be different in every step, which is usually realized by the coin operator being in some way dependent on t .

1.1 Quantum walks in one dimension

Let us now move to the specific cases of quantum walks on an infinite line, finite line and on a circle. This section will start with the infinite line and then continue to explain the changes for the finite cases. The concept of lazy walk will then also be briefly introduced.

Both the line and the circle are 2-regular graphs, so it is possible to formulate the Hilbert space of the walk as in (1.6). The position and the coin spaces for an infinite line are defined as follows

$$\mathcal{H}_p = \{|m\rangle | m \in \mathbb{Z}\}, \quad \mathcal{H}_c = \{|L\rangle, |R\rangle\}, \quad (1.14)$$

so the whole Hilbert space is then equal to

$$\mathcal{H} = \{|m\rangle \otimes |L\rangle \equiv |m, L\rangle, |m\rangle \otimes |R\rangle \equiv |m, R\rangle | m \in \mathbb{Z}\}. \quad (1.15)$$

The most commonly used two-dimensional coin is probably the Hadamard coin

$$H = \frac{1}{\sqrt{2}} \begin{pmatrix} 1 & 1 \\ 1 & -1 \end{pmatrix}, \quad (1.16)$$

which is an example of a balanced coin and will also be mostly used through out this whole work. There are of course other options, however it turns out that most coin operators generate equivalent evolutions [16]. This phenomenon will be discussed later, for now the focus will move to the shift operator. The flip-flop operator in this case looks like

$$S^{FL} = \sum_{m \in \mathbb{Z}} |m+1, L\rangle\langle m, R| + |m-1, R\rangle\langle m, L|. \quad (1.17)$$

However, another intuitive shift operator can be defined in this case and that is the continuing shift operator mentioned earlier

$$S = \sum_{m \in \mathbb{Z}} |m+1, R\rangle\langle m, R| + |m-1, L\rangle\langle m, L|, \quad (1.18)$$

where the walker just continues in the same direction and does not turn around. This will also be the main choice of the shift operator for the duration of this work. The example of the difference of the evolution between the classical and quantum walk with the continuing shift operator and different initial coin states can be seen in Fig. 1.1.

To get the description of the walk on a finite line and on a circle, the only necessary thing is to modify the shift operator by adding boundary conditions. For a circle of length N one simply adds periodic boundary condition represented by identifying $N \equiv 0$

$$S^{circle} = \sum_{m=0}^{N-2} |m+1, R\rangle\langle m, R| + |0, R\rangle\langle N-1, R| + \sum_{m=1}^{N-1} |m-1, L\rangle\langle m, L| + |N-1, L\rangle\langle 0, L|. \quad (1.19)$$

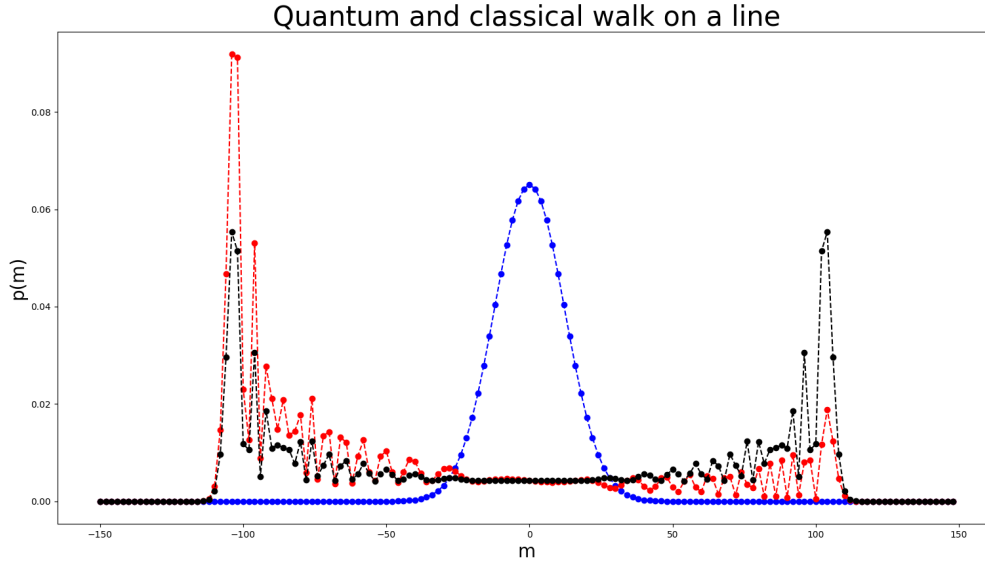


Figure 1.1: First 150 steps of the Hadamard walk on a line with the continuing shift operator and different initial coin states versus the first 150 steps of a classical walk with a balanced coin. All walkers started at the origin, the blue line is the classical walker, the red line is the quantum walker with initial coin state $|L\rangle$ and the black line is the quantum walker with initial coin state $|L\rangle + i|R\rangle$.

There is also an option of generalizing this shift operator by adding some phases to the walker when crossing the origin $|0\rangle$. For the finite line the boundary condition is reflecting, i.e. the shift operator looks like

$$S^{finite} = \sum_{m=0}^{N-2} |m+1, R\rangle\langle m, R| + |N-1, L\rangle\langle N-1, R| + \sum_{m=1}^{N-1} |m-1, L\rangle\langle m, L| + |0, R\rangle\langle 0, L|. \quad (1.20)$$

So the walker stays in place and turns around at the end of the line. There is again also a more general option to give the walker some local phase during the reflection as will be shown in the next chapter.

For the finite line there are more options, another one is to place absorbing boundaries at either one end or both ends of the finite line. Assuming $|0\rangle$ is an absorbing point, projector

$$\Pi = 1 - |0\rangle\langle 0|, \quad (1.21)$$

is simply added after every step of the walk, so that

$$|\psi(t+1)\rangle = \Pi U |\psi(t)\rangle. \quad (1.22)$$

This however yields a non-unitary evolution. If one wants to keep the evolution unitary, another option is the following. After every step there is a projection measurement M_0 which acts on the state of the walker $|\psi\rangle$ in the following way

$$M_0 |\psi\rangle = \begin{cases} |0\rangle & \dots \text{ with probability } |\langle\psi|0\rangle|^2, \\ \frac{|\psi\rangle - \langle 0|\psi\rangle |0\rangle}{\sqrt{1 - |\langle\psi|0\rangle|^2}} & \dots \text{ with probability } 1 - |\langle\psi|0\rangle|^2. \end{cases} \quad (1.23)$$

In case the particle is in the state $|0\rangle$ after the measurement, the walk is finished. This kind of walk with absorbing boundaries was considered in [17] where the absorption probabilities have been calculated for several different cases. Important result however is the fact that while the probability of absorption is always 0 or 1 in the classical case, in the quantum case there are major differences.

As has been said earlier, for the classical random walks there is an existing limit via the lazy walk from discrete to continuous time case. While the limit cannot be done in the same way for the quantum walk, the lazy walk can still be defined. Moreover, it was already proved to have some interesting influence for example on speeding up the search algorithms based on quantum walks [18–21]. The lazy quantum walk is usually defined in literature as a process of adding self-loops to all vertices of the graph. This self-loops represent the possibility of the walker to stay in place. Generally, it is necessary to add one more base state $|S\rangle$ into the local coin spaces and also to change the original shift operator S in the following way

$$S^{lazy} = S + \sum_{m \in \mathbb{Z}} |m, S\rangle\langle m, S|. \quad (1.24)$$

The coin operator then needs to be changed as well since the dimension of the coin space has increased. For quantum walk in one dimension the local coin spaces are now three dimensional and the usual choice of coin is not the Hadamard coin anymore, but the Grover coin operator

$$G_3 = \frac{1}{3} \begin{pmatrix} -1 & 2 & 2 \\ 2 & -1 & 2 \\ 2 & 2 & -1 \end{pmatrix}, \quad (1.25)$$

where more about Grover operator and its origin will be explained later.

1.2 Coin operator and equivalence classes

The coin operator is defined as an arbitrary unitary operation on the coin degrees of freedom, so how does one choose a coin operator, is the question. For two-dimensional coin space the commonly most used coin operator has already been introduced as the Hadamard coin (1.16). For the lazy walk the Grover coin, inspired by the Grover search operator [22], has been introduced as well as (1.25) for the three-dimensional coin spaces. The Grover coin is actually defined for an arbitrary dimension d as

$$G = 2 |\psi_S\rangle\langle\psi_S| - I, \quad (1.26)$$

where $|\psi_S\rangle$ denotes the normalized equal superposition of coin states corresponding to the given vertex

$$|\psi_S\rangle = \frac{1}{\sqrt{d}} \sum_{i=1}^d |i\rangle. \quad (1.27)$$

Another widely used coin, suitable for arbitrary dimension d of the vertex subspaces, is the Fourier coin, which is basically just an operator of the quantum discrete Fourier transform defined as

$$DFT = \frac{1}{\sqrt{d}} \begin{pmatrix} 1 & 1 & 1 & \dots & 1 \\ 1 & \omega & \omega^2 & \dots & \omega^{d-1} \\ & & & \ddots & \\ 1 & \omega^{d-1} & \omega^{2(d-1)} & \dots & \omega^{(d-1)(d-1)} \end{pmatrix}, \quad \text{where } \omega = e^{2\pi i/d}. \quad (1.28)$$

Describing and working with arbitrary unitary operators in higher dimension can be quite difficult. However, for the two-dimensional coin space the general coin operator is an arbitrary member of the $SU(2)$ group and can be parametrized as

$$C = e^{i\delta} e^{-i\psi\sigma_z/2} e^{-i\theta\sigma_y/2} e^{-i\phi\sigma_z/2}, \quad \text{where } \gamma, \psi, \theta, \phi \in \mathbb{R}. \quad (1.29)$$

It is a parametrization by the Euler angles ψ, θ, ϕ with the addition of a global phase δ . The global phase does not influence the quantum evolution and can be omitted. However, Euler angles represent the rotations of the spinor in \mathbb{R}^3 , rotations around different axes x, y , and z are represented as

$$R_x(\theta) \equiv e^{-i\theta\sigma_x/2}, \text{ resp. } R_y(\theta) \equiv e^{-i\theta\sigma_y/2}, \text{ resp. } R_z(\theta) \equiv e^{-i\theta\sigma_z/2}, \quad (1.30)$$

where σ_x, σ_y a σ_z are Pauli matrices. So with this parametrization the C operator rotates the state on the Bloch sphere by the angle θ around some axis \mathbf{r} .

There seems to be still quite a lot of options for the choice of the coin even in two dimensions. Luckily, it turns out that in many cases the evolutions of the one-particle quantum walks in one dimension will be equivalent. In the rest of this section the results of [16] concerning these equivalences will be summarized.

The first thing that needs to be clarified is what exactly is meant by the coin operators being unitary equivalent. For operators that generally means that U and U' are **unitary equivalent**, if there exists an unitary V such that

$$U' = VUV^\dagger. \quad (1.31)$$

For quantum evolution of some initial state $|\psi(0)\rangle \in \mathcal{H}$ this means

$$|\psi(t)\rangle = U^t |\psi(0)\rangle = (V^\dagger U' V)^t |\psi(0)\rangle = V^\dagger U'^t V |\psi(0)\rangle. \quad (1.32)$$

Measuring any observable A of a quantum system with initial state $|\psi(0)\rangle$ after t steps under U will yield the same statistic as measuring the rotated observable VUV^\dagger in the system with initial state $V|\psi(0)\rangle$ after t steps under U' . So the dynamic of the state $|\psi(0)\rangle$ under U will be the same as the dynamic of $V|\psi(0)\rangle$ under U' .

This still leaves quite a large number of possible equivalences. However, there are some additional requirements in case of systems representing quantum walks, these bring the number down. First of all, it is necessary for the new unitary operator U' to keep the shape $U' = S'C'$. Considering only the case of the quantum walk on a line with the same local coin operator C on every vertex allows following changes of operators

$$\begin{aligned} S &= \sum_{m \in \mathbb{Z}} |m+1, R\rangle\langle m, R| + |m-1, L\rangle\langle m, L| \\ &\rightarrow S' = \sum_{m \in \mathbb{Z}} |m+1, R'\rangle\langle m, R'| + |m-1, L'\rangle\langle m, L'|, \\ C = I \otimes C &\rightarrow C' = I \otimes C', \end{aligned}$$

where $\{|R'\rangle, |L'\rangle\}$ is the new canonical basis of the local coin spaces.

One important property of the shift operator (1.18) is its translation invariance. So that is one property that can be required to be preserved. Next, one will usually require the entanglement between the coin and the walker not to be affected by the transformation V . This means V must be of the following shape

$$V = W \otimes X. \quad (1.33)$$

One more example of such additional requirement can be that the canonical basis $\{|R\rangle, |L\rangle\}$ of the coin space must not change under X .

Lets consider the case when the requirements are to preserve entanglement and for X not to alter the coin canonical basis¹. It then turns out that the original three-parameter family of evolution operator reduces to one-parameter real-valued family of local coin operators [16]

$$C = e^{i\frac{\phi}{2}\sigma_y} = \begin{pmatrix} \cos\left(\frac{\phi}{2}\right) & -\sin\left(\frac{\phi}{2}\right) \\ \sin\left(\frac{\phi}{2}\right) & \cos\left(\frac{\phi}{2}\right) \end{pmatrix}. \quad (1.34)$$

This class of operators is equivalent, according to the chosen requirements, to

$$C' = \begin{pmatrix} \cos\left(\frac{\phi}{2}\right) & \sin\left(\frac{\phi}{2}\right) \\ \sin\left(\frac{\phi}{2}\right) & -\cos\left(\frac{\phi}{2}\right) \end{pmatrix}, \quad \pi \in [0, \pi], \quad (1.35)$$

which can be rewritten, using parametrization $\rho = \cos\left(\frac{\phi}{2}\right)$, to

$$C' = \begin{pmatrix} \rho & \sqrt{1-\rho^2} \\ \sqrt{1-\rho^2} & -\rho \end{pmatrix}, \quad \rho \in [0, 1]. \quad (1.36)$$

This class now also directly contains the Hadamard coin for $\rho = 1/2$. The equivalence transformation for these two classes is equal to

$$V = \sum_{m \in \mathbb{Z}} e^{-i\pi j} |m\rangle\langle m| \otimes e^{-i\frac{\pi}{4}\sigma_z}. \quad (1.37)$$

The option of preserving translation invariance of the shift operator and the entanglement of the walker-coin system is also discussed in [16]. This time the invariance of the canonic basis of the coin state is not required. For $W = I$ and a special choice of X , which rotates the rotation axis \mathbf{r} of the Bloch sphere representation to the vertical position,

$$C \rightarrow X C X^\dagger = e^{i\frac{\phi}{2}\sigma_z}. \quad (1.38)$$

So the resulting equivalence class is also one-parametric and corresponds to the rotation of the coin around the z -axis.

1.3 Solution using Fourier transform

There are more methods to analyze the properties of the quantum walk on a line, the one using Fourier transform will now be summarized here [23]. The reason for the Fourier transform being helpful in this case is the translation invariance of the walk. As a result, a very simple description of the walk exists in the Fourier space. The focus will now be on the case of the infinite line and the special choice of the Hadamard coin. Later, the modification for the general coin of the form (1.36) and the case of the circle will be discussed.

The Hadamard walk described above can be rewritten into the following recurrent form (difference equation)

$$\begin{aligned} \psi(x, t+1) &= \frac{1}{\sqrt{2}} \begin{pmatrix} 1 & 1 \\ 0 & 0 \end{pmatrix} \psi(x+1, t) + \frac{1}{\sqrt{2}} \begin{pmatrix} 0 & 0 \\ 1 & -1 \end{pmatrix} \psi(x-1, t) \\ &= M_+ \psi(x+1, t) + M_- \psi(x-1, t), \quad \forall x \in \mathbb{Z}, \end{aligned} \quad (1.39)$$

¹So, the translation invariance is not required.

where M_+ and M_- will be defined similarly even for the general shape of the coin (1.36). Here $\boldsymbol{\psi}(x, t)$ is the vector of amplitudes corresponding to the two different coin states

$$\boldsymbol{\psi}(x, t) = \begin{pmatrix} \psi_L(x, t) \\ \psi_R(x, t) \end{pmatrix}. \quad (1.40)$$

The Fourier transform of the amplitudes in the position space is defined as the transformation of functions $\psi : \mathbb{Z} \rightarrow \mathbb{C}^2$ to functions $\tilde{\psi} : [-\pi, \pi] \rightarrow \mathbb{C}^2$. The later are defined as

$$\tilde{\psi}(k, t) = (F\psi)(k, t) = \sum_{x=-\infty}^{\infty} e^{ikx} \psi(x, t), \quad (1.41)$$

and the corresponding inverse transport is then given as

$$\psi(x, t) = \frac{1}{2\pi} \int_{-\pi}^{\pi} \tilde{\psi}(k, t) e^{-ikx} dk. \quad (1.42)$$

To avoid confusion, the previous definitions hold for the individual components ψ_R and ψ_L of the amplitude vector $\boldsymbol{\psi}$. The recurrence relation (1.39) in the Fourier space is then

$$\tilde{\boldsymbol{\psi}}(k, t+1) = (e^{ik} M_+ + e^{-ik} M_-) \tilde{\boldsymbol{\psi}}(k, t) = M_k \tilde{\boldsymbol{\psi}}(k, t), \quad \forall k \in [-\pi, \pi], \quad (1.43)$$

where M_k can be generally described for any local unitary coin operator C as

$$M_k = \begin{pmatrix} e^{-ik} & 0 \\ 0 & e^{ik} \end{pmatrix} C. \quad (1.44)$$

It is also obvious that as a product of two unitary matrices, M_k is also generally a unitary matrix.

It is now visible how much did the recurrence relation simplified, in the Fourier space one gets

$$\tilde{\boldsymbol{\psi}}(k, t) = M_k^t \tilde{\boldsymbol{\psi}}(k, 0), \quad \forall k \in [-\pi, \pi], \quad (1.45)$$

where M_k is now easy to diagonalize. Denoting the eivenvectors of M_k as $\{\boldsymbol{\phi}_k^1, \boldsymbol{\phi}_k^2\}$ and the corresponding eigenvalues as $\{\lambda_k^1, \lambda_k^2\}$, the evolution in the Fourier space can be obtained as

$$\tilde{\boldsymbol{\psi}}(k, t) = (\lambda_k^1)^t \langle \boldsymbol{\phi}_k^1 | \tilde{\boldsymbol{\psi}}(k, 0) \rangle \boldsymbol{\phi}_k^1 + (\lambda_k^2)^t \langle \boldsymbol{\phi}_k^2 | \tilde{\boldsymbol{\psi}}(k, 0) \rangle \boldsymbol{\phi}_k^2, \quad \forall k \in [-\pi, \pi]. \quad (1.46)$$

The eigenvalues can be rewritten as $\lambda_k^1 = e^{-i\omega_k}$ and $\lambda_k^2 = e^{i(\omega_k+\pi)}$, where $\omega_k \in [-\pi/2, \pi/2]$ can be determined from the relation $\sin(\omega_k) = \sin(k)/\sqrt{2}$.

For the Hadamard walk the resulting eigenvectors are equal to

$$\boldsymbol{\phi}_k^1 = \frac{1}{\sqrt{N_-}} \begin{pmatrix} e^{-ik} \\ \sqrt{2}e^{-i\omega_k} - e^{-ik} \end{pmatrix}, \quad \boldsymbol{\phi}_k^2 = \frac{1}{\sqrt{N_+}} \begin{pmatrix} e^{-ik} \\ -\sqrt{2}e^{-i\omega_k} - e^{-ik} \end{pmatrix}, \quad (1.47)$$

where

$$N_{\mp} = 2 \left(1 + \cos^2(k) \mp \cos(k) \sqrt{1 + \cos^2(k)} \right). \quad (1.48)$$

For the walker with the initial state $|\psi(t)\rangle = |0, L\rangle$ the final result consists of the following integrals

$$\begin{aligned} \psi_L(n, t) &= \frac{1 + (-1)^{n+t}}{2} \int_{-\pi}^{\pi} \frac{dk}{2\pi} \left(1 + \frac{\cos(k)}{\sqrt{1 + \cos^2(k)}} \right) e^{-i(\omega_k t + kn)}, \\ \psi_R(n, t) &= \frac{1 + (-1)^{n+t}}{2} \int_{-\pi}^{\pi} \frac{dk}{2\pi} \frac{e^{ik}}{\sqrt{1 + \cos^2(k)}} e^{-i(\omega_k t + kn)}. \end{aligned} \quad (1.49)$$

This kind of integrals are not easy to evaluate, but the asymptotic evolution can be obtained, for further details the reader is referred e.g. to the aforementioned [23]. Final eigenvalues and eigenvectors of M_k for a general coin of the shape (1.36) can be found in [24]. The eigenvalues of M_k turn out to be of the same shape, just the frequencies ω_k are given by

$$\sin(\omega_k) = \sqrt{\rho} \sin(k). \quad (1.50)$$

So the general procedure to get the time evolution of the probability amplitudes for the quantum walk on the line is as follows. First, the amplitudes of the initial state $\psi(x, 0)$ have to be transformed via (1.41) into the Fourier space picture. Next, the transformed initial state is inserted into (1.46) in order to obtain the final amplitudes in the time t in Fourier space. Finally, the obtained amplitudes have to be again transformed back using the inverse Fourier transform (1.42). The inverse Fourier transform is usually the problematic part of this procedure, because the resulting integrals are not easy to solve. However, there exists quite a well developed theory concerned with investigating the asymptotic expansion of integrals, so one can say something about the properties of the amplitudes for large times t .

Fourier transform can also be helpful in the case of the circle, since in that case the problem is also translation invariant. The Fourier transform (1.41) will now turn into the discrete Fourier transform (1.28), which for the amplitudes has the following definition

$$\tilde{\psi}(k, t) = (F\psi)(k, t) = \frac{1}{\sqrt{N}} \sum_{x=0}^{N-1} e^{ikx} \psi(x, t). \quad (1.51)$$

The procedure to obtain the solution will be almost the same as in the case of the infinite line, just with a different definition of Fourier transform. The evolution will again be given by

$$\tilde{\psi}(k, t) = M_k^t \tilde{\psi}(k, 0), \quad \forall k \in [-\pi, \pi], \quad (1.52)$$

where M_k will again be an unitary matrix, just of a slightly different shape. So it is again necessary to find its eigenvalues and eigenvectors in order to follow the general procedure described above. The frequencies $\omega_k^{(N)}$ are now given by [24]

$$\sin(\omega_k^{(N)}) = \sqrt{\rho} \sin(2\pi k/N), \quad (1.53)$$

for the general coin of the shape from the equation (1.36).

As to why are the relationships for determining the frequencies ω_k and $\omega_k^{(N)}$ especially mentioned here, lets have a look on [25]. The main concern of [25] is to generalize the concept of *hitting time* in classical random walks to the quantum case. In the classical case this term is defined as the average time the walker needs to reach the final point from for the first time starting from the given initial position. There exists several attempts to generalize this concept to the quantum case, usually involving some probability thresholds and partial measurements. Since there are drawbacks to both, the general idea of [25] is to find an alternative definition. They define the notion of *group velocity based hitting time* which is based on the following intuitive thought process. Lets suppose the walker carries some information and one has to wait for the information to reach the given vertex. The information travels in some environment (which is passive due to the unitary evolution) and the signal velocity then should be the maximum group velocity. The group velocity of the quantum walker on the line is then defined as

$$v_g = \frac{d\omega}{dk}, \quad (1.54)$$

where ω are the frequencies from the Fourier transform taken as functions of k . In both cases ω_k and $\omega_k^{(N)}$ depend on the parameter ρ of the general equivalence class and so the group velocity will as well. That suggests the coin parameter ρ is related to the rate with which the excitation spreads through the system.

Chapter 2

Asymptotic evolution and percolated quantum walks

This chapter explains the concept of quantum walks on dynamically percolated graphs and their asymptotic evolution in detail. It will also focus more in detail on the results for one walker in one dimension, for normal and also for a lazy walker.

Let us first take a look at what exactly is meant when one talks about dynamically percolated graph. It is a graph whose edges can get randomly broken and reappear again during the time evolution of the system. Focusing on just one edge $(v_1, v_2) \in E$ of the graph $G(E, V)$, there is an assigned probability p_{12} with which the edge will be considered broken, i.e. $(v_1, v_2) \notin K$, where $K \subset E$ is the new configuration of edges, in the current step of the evolution. The set of vertices stays the same the whole time. There are sometimes just no edges connected to the vertex. There are such probabilities of the edge being broken for all edges of the original graph $G(E, V)$. For the quantum walker it means that every step of the walk can take place on a different subgraph of $G(E, V)$, i.e. on different configuration of edges. The probability of a certain configuration K appearing is then given as

$$p_K = \prod_{(v_i, v_j) \in K} \prod_{(v_k, v_l) \notin K} (1 - p_{ij}) p_{kl}, \quad (2.1)$$

where $p_{ab}, \forall v_a, v_b \in V$ is the probability of the edge (v_a, v_b) being broken. Not surprisingly the sum of the probabilities of all possible configurations appearing is equal to one

$$\sum_K p_K = 1. \quad (2.2)$$

Now lets take a look at how this evolution can be described by evolution operators. The possibility of different configurations of edges results in an associated unitary evolution operators U_K . So in every step of the evolution one of these unitary operations is randomly applied according to the probability distribution p_K . For quantum walks the evolution operator consists of the shift operator S and the coin operator C . The Hilbert space of the walker stays the same, but it is necessary to somehow express the broken edges. This is done by changing the shift operator. More specifically, the shift operator is modified, so that it no longer allows the walker to move along the broken edges. Here only one specific way will be shown for the one dimensional case, however, the reader should be aware that different approaches are also possible, e. g. as in [7].

For a walker on a finite line let us first take a look at the original (non-percolated) continuing shift operator S

$$S = \sum_{m=0}^{N-2} |m+1, R\rangle\langle m, R| + \mathcal{R}|N-1, R\rangle\langle N-1, R| + \sum_{m=1}^{N-1} |m-1, L\rangle\langle m, L| + \mathcal{R}|0, L\rangle\langle 0, L|, \quad (2.3)$$

where the end of a line is treated as a broken edge and the local reflection operator \mathcal{R} is applied. For the circle the non-percolated shift operator is

$$S = \sum_{m=0}^{N-2} |m+1, R\rangle\langle m, R| + |0, R\rangle\langle N-1, R| + \sum_{m=1}^{N-1} |m-1, L\rangle\langle m, L| + |N-1, L\rangle\langle 0, L|, \quad (2.4)$$

where periodic boundary conditions have been applied to both ends. The modified shift operator for a given configuration K is then defined as

$$S_K = \sum_{(m,m+1) \in K} |m+1, R\rangle\langle m, R| + \sum_{(m-1,m) \in K} |m-1, L\rangle\langle m, L| + \sum_{(m,m+1) \notin K} \mathcal{R}|m, R\rangle\langle m, R| + \sum_{(m-1,m) \notin K} \mathcal{R}|m, L\rangle\langle m, L|, \quad (2.5)$$

where \mathcal{R} is the local reflection operator

$$\mathcal{R} = \begin{pmatrix} 0 & e^{i\beta} \\ e^{i\alpha} & 0 \end{pmatrix}, \quad \alpha, \beta \in \mathbb{R}. \quad (2.6)$$

This means that if there is no edge, the walker stays in place. He only turns around (the coin switches) while possibly obtaining some local phase. The following text will however be focused mainly on the special case of the reflection operator without any additional phases where

$$\mathcal{R} = \begin{pmatrix} 0 & 1 \\ 1 & 0 \end{pmatrix} = \sigma_x. \quad (2.7)$$

In summary, while the coin operator stays the same, the shift operator is modified according to the given edge configuration. The unitary evolution operator for a given configuration of edges will then be $U_K = S_K C$.

2.1 Asymptotic evolution

The concept of finite dimensional systems with random unitary operations (RUOs) and their asymptotic evolution is more general than just the special case of quantum walks on percolated graphs. The following description will follow the results mainly from [10] where more details and proofs can be found.

Random unitary operation Φ is generally defined as a completely positive trace-preserving map which can be decomposed into

$$\Phi(\rho) = \sum_i p_i U_i \rho U_i^\dagger. \quad (2.8)$$

Here $\{U_i\}_i$ is a set of unitary operations acting on a given Hilbert space of the system \mathcal{H} , ρ is a density matrix representing the state of the quantum system and p_i is a probability distribution such that $p_i > 0$, $\forall i$ and $\sum_i p_i = 1$. One can notice that this is a classical probability distribution, which represents

the classical uncertainty about the random choice of unitary operation in that particular step. This can generally represent some kind of error-creating outside processes which change the evolution of the system. The superoperator Φ acts on the space $\mathcal{B}(\mathcal{H})$, which is a Hilbert space of all linear operators acting on \mathcal{H} . The evolution of the quantum system is then defined as an iterative application of the superoperator Φ on the initial state of the system $\rho(0)$, so after $t \in \mathbb{N}$ steps of the evolution the state of the system will be

$$\rho(t) = \Phi^t(\rho(0)) = \Phi(\Phi(\dots\Phi(\rho(0))))). \quad (2.9)$$

Since $\mathcal{B}(\mathcal{H})$ truly is a Hilbert space, scalar product can be defined on it. More specifically in this case the Hilbert-Schmidt scalar product which is defined as

$$\langle A, B \rangle_{HS} = \text{Tr}[A^\dagger B], \quad \forall A, B \in \mathcal{B}(\mathcal{H}). \quad (2.10)$$

The adjoint operator related to this scalar product is then

$$\Phi^\dagger(\rho) = \sum_i p_i U_i^\dagger \rho U_i. \quad (2.11)$$

It is important to point out that generally Φ is neither hermitian nor normal (so also not unitary). This means that it can be impossible to diagonalize. However, one can still say quite a lot about the iterated evolution using the Jordan normal forms.

Let us now very briefly recapitulate what exactly are Jordan normal forms, so it is later more clear what exactly are the later introduced attractors. For every complex square matrix A of size $n \times n$ there exists such a basis, in which A will have a block diagonal shape

$$\tilde{A} = \begin{pmatrix} J_1 & & \\ & \ddots & \\ & & J_r \end{pmatrix}, \quad (2.12)$$

where $J_i, i \in \{1, \dots, r\}$ are Jordan blocks of the shape

$$J_i = \begin{pmatrix} \lambda_i & 1 & & \\ & \lambda_i & 1 & \\ & & \ddots & 1 \\ & & & \lambda_i \end{pmatrix}. \quad (2.13)$$

Block sizes are the geometric multiplicities of the eigenvalue λ_i . This also means that it is possible to find such a matrix P , that $A = P\tilde{A}P^{-1}$. For all λ_i it is possible to find such an vector $x_{i, \dim(J_i)}$, so that

$$(A - \lambda_i I)^{\dim(J_i)} x_{i, \dim(J_i)} = 0. \quad (2.14)$$

For $\dim(J_i) > 1$ this vector is then called generalized eigenvector, for $\dim(J_i) = 1$ it is clearly simply an eigenvector, together with other vectors x for which

$$(A - \lambda_i I)^n x = 0, \quad n \leq \dim(J_i). \quad (2.15)$$

Back to the superoperator Φ , it can be shown (among other things) that if $\lambda \in \mathbb{C}$ is an eigenvalue of Φ , then $|\lambda| \leq 1$. Also, if X_λ is a generalized eigenvector of Φ corresponding to the eigenvalue λ , then either $\lambda = 1$, or $\text{Tr}(X_\lambda) = 0$. Additionally, all of the generalized eigenvectors corresponding to such eigenvalues for which $|\lambda| = 1$ are eigenvectors, so the dimension of their Jordan blocks is 1. However, the most important thing is an interesting fact about the decomposition of the initial state of the system

ρ into the Jordan basis. Quite an important thing can actually be shown about the coefficients of the decomposition. All of the coefficients corresponding to eigenvalues for which $|\lambda| < 1$ go to zero in the limit of large amount of applications of Φ . So in the asymptotic limit only the eigenvectors corresponding to the eigenvalues for which $|\lambda| = 1$ are of interest, these will be called **attractors**.

Then the **attractor space** of the superoperator Φ can be defined as

$$\text{Atr}(\Phi) = \bigoplus_{\lambda \in \sigma_{|1|}} \text{Ker}(\Phi - \lambda I), \quad (2.16)$$

where $\sigma_{|1|}$ denotes the set of eigenvalues of Φ with absolute value equal to 1. Based on this definition, it can be also shown that

$$\text{Ker}(\Phi - \lambda I) = \{X \in \mathcal{B}(\mathcal{H}) \mid U_i X U_i^\dagger = \lambda X, \quad \forall i\}. \quad (2.17)$$

This reveals a constructive way how to obtain the attractors of the superoperator Φ , which will be used later in this chapter.

Defining the projector $\mathcal{P} : \mathcal{B}(\mathcal{H}) \rightarrow \text{Atr}(\Phi)$ as

$$\mathcal{P}(\cdot) = \sum_{\lambda \in \sigma_{|1|}, i} \lambda \text{Tr}[X_{\lambda, i}^\dagger \cdot] X_{\lambda, i}, \quad (2.18)$$

where index i represents different orthonormal attractors corresponding to the same eigenvalue λ , the asymptotic state $\rho_\infty(t)$ of the system with the initial state $\rho(0)$ for $t \gg 1$ can be denoted as

$$\rho_\infty(t) = \sum_{\lambda \in \sigma_{|1|}, i} \lambda^t \text{Tr}[X_{\lambda, i}^\dagger \rho(0)] X_{\lambda, i}. \quad (2.19)$$

It is important to notice, that the final asymptotic state does not depend on the probability distribution p_K at all. However, the speed of convergence towards this state might. Another thing which can be seen from the formula (2.19) is that the asymptotic state does not necessarily need to be stationary, it can be periodic or even non-periodic and non-stationary. The asymptotic state will be stationary only in case 1 is the only eigenvalue present.

There are also another two properties of attractors which one might find useful. First, the product of two attractors X_1 and X_2 corresponding to the eigenvalues λ_1 and λ_2 is either also an attractor $X_1 X_2$ corresponding to the eigenvalue $\lambda_1 \lambda_2$, or a zero operator. Second, if X is an attractor corresponding to the eigenvalue λ , then X^\dagger is an attractor corresponding to the eigenvalue λ^* . While working with orthonormal sets of attractors for all eigenvalues as in (2.19), it also holds that

$$\langle X_{\lambda_1, i}, X_{\lambda_2, j} \rangle_{HS} = \text{Tr}[X_{\lambda_1, i}^\dagger X_{\lambda_2, j}] = \delta_{\lambda_1 \lambda_2} \delta_{ij}. \quad (2.20)$$

These results can also be obtained via a different road using the argument of von Neumann entropy as in [26]. In short, looking at the von Neumann entropy $S(\rho) = -\text{Tr}(\rho \ln \rho)$, one can show that

$$S(\Phi(\rho)) \geq \sum_K p_K S(U_K \rho U_K^\dagger) = S(\rho). \quad (2.21)$$

So in addition to being bounded, the entropy is also monotonous for finite dimensional systems. This indicates existence of constant entropy in the limit of large enough number of iterations.

Returning back to the quantum walks in one dimension, lets take a look at how does the search for attractors looks like in these kinds of systems. The condition (2.17) will now be of utter importance. The random unitary operators can be written in the form $U_K = S_K C$, so the condition from (2.17) on attractors corresponding to the eigenvalue λ becomes

$$S_K C X C^\dagger S_K^\dagger = \lambda X, \quad \forall K \subset E. \quad (2.22)$$

Taking into account the special case of the shift operator (2.62) and considering the case of an empty configuration, i.e. no edges present, one obtains

$$RCX(RC)^\dagger = \lambda X. \quad (2.23)$$

Here R is a global reflection operator, where the walker only turns around all the time while staying in place

$$R = \sum_i \mathcal{R}|i, R\chi i, R\rangle + \mathcal{R}|i, L\chi i, L\rangle. \quad (2.24)$$

The equation (2.23) is called the **coin condition**. What is interesting (and useful) about it is its block structure. Both R and C have a block structure in the context of vertex subspaces. Lets split the attractor X into vertex blocks

$$X_b^a \equiv \langle a|X|b\rangle, \quad \forall a, b \in V, \quad (2.25)$$

then the coin condition for the vertices reads

$$\mathcal{R}C_{v_1} X_{v_2}^{v_1} C_{v_2}^\dagger \mathcal{R}^\dagger = \lambda X_{v_2}^{v_1}, \quad (2.26)$$

where C_a denotes the local coin operator on the vertex $a \in V$. This condition can be equivalently reformulated into a simple eigenvector search of the form

$$[\mathcal{R}C_{v_1} \otimes (\mathcal{R}C_{v_2})^*] x_{v_2}^{v_1} = \lambda x_{v_2}^{v_1}, \quad (2.27)$$

where $\langle c, d|x_{v_2}^{v_1}\rangle = \langle c|X_{v_2}^{v_1}|d\rangle$ with $|c\rangle, |d\rangle$ being the coin states on vertices v_1, v_2 respectively. Through these conditions one can obtain the possible blocks of the attractor. However, these still need to be joined somehow to form the whole attractor.

The way to build an attractor from the obtained blocks is provided by the **shift conditions**. Rewriting the equation (2.22) as

$$CXC^\dagger = \lambda S_K^\dagger X S_K, \quad \forall K \subset E, \quad (2.28)$$

it becomes obvious, that since the left side is the same for all configurations, the right one must be also. From that directly follow the shift conditions

$$S_K^\dagger X S_K = S_L^\dagger X S_L, \quad K, L \subset E. \quad (2.29)$$

Even though this split of the original condition provides a more constructive way of looking for attractors, it is still in most cases quite a non-trivial problem. There is however a certain special subset of attractors for which the problem simplifies significantly. First, one needs to find the **common eigenstates** of all the possible unitary operators, i.e.

$$U_K |\phi_\alpha\rangle = \alpha |\phi_\alpha\rangle, \quad \forall K \subset E, \alpha \in \mathbb{C}. \quad (2.30)$$

Then an arbitrary linear combination of the form

$$Y_\lambda = \sum_{\lambda=\alpha\beta^*} A_{\beta,j}^{\alpha,i} |\phi_{\alpha,i}\rangle \langle \phi_{\beta,j}|, \quad (2.31)$$

is an attractor with eigenvalue $\lambda = \alpha\beta^*$. In the formula above $A_{\beta,j}^{\alpha,i} \in \mathbb{C}$ are the linear coefficients and indices i, j denote different common eigenstates related to the same eigenvalue. Attractors of this kind

are called the **p-attractors** and they are usually easier to find, because finding common eigenstates is simpler due to the reduced dimensionality of the problem.

For common eigenstates one can actually obtain the coin condition of the form

$$RC|\phi_\alpha\rangle = \alpha|\phi_\alpha\rangle, \quad (2.32)$$

and also the corresponding shift conditions

$$S_K^\dagger|\phi_\alpha\rangle = S_L^\dagger|\phi_\alpha\rangle, \quad \forall K, L \subset E. \quad (2.33)$$

in a very similar way as it has been done earlier for the general attractors. Through these the possible parts of the common eigenstate corresponding to the vertex subspaces are first obtained and then put together using the shift conditions.

In many cases of interest the only non-p-attractor is identity I , which is always present, and in that case the only problem is then to prove this. However, there can also be other non-p-attractors present and in that case the problem of finding them can become quite non-trivial.

The last note, before continuing onto the actual example solutions for a walker in one dimension, is about dealing with walks on arbitrary graphs. So far the description for the walker in one dimension followed the formalism used for example in [27] or [28]. However, for graphs of higher degrees it might become quite impractical. For a line or for a two-dimensional lattice the continuing shift operator and also the local reflection operator is easy and intuitive to define. In case of a general graph, it is however not so straightforward. For example in [7–9] and also [29] the flip-flop shift operator R_K^{FL} is used instead, meaning the walker moves in the direction of the coin to the next vertex and then turns back into the direction of the original one. Also in this case the reflection operator is omitted completely and the walker only stays in place and does not move, even in the coin degree of freedom, in case of a broken edge, effectively the local identity is applied. This shift-operator can then be generalized by adding a permutations of coin states at the vertices P . The whole unitary operator is then $U_K^{FL} = PR_K^{FL}C$, where the new shift-operator is defined as $S_K^{FL} = PR_K^{FL}$. The coin condition then reads

$$(CP)^\dagger XCP = \lambda X, \quad (2.34)$$

and the shift conditions become

$$R_K^{FL}X(R_K^{FL})^\dagger = R_L^{FL}X(R_L^{FL})^\dagger, \quad \forall K, L \subset E. \quad (2.35)$$

So basically other shift operators are equivalent to the change of the coin operator. In [7] and the others the coin is actually applied first, so $U_K^{FL} = CPR_K^{FL}$, but the equivalence of these approaches is also explained there in section II.C.. It turns out that the only difference is the change of the initial state.

For the line, and subsequently also for the two-dimensional regular lattice, and the choice of the local reflection operator $\mathcal{R} = e^{i\alpha}\sigma_x$, $\alpha \in \mathbb{R}$ the approaches are actually equivalent. In these cases the only possible permutation of the coin states on the vertices is the global reflection operator R (switching the coins on all vertices). After some thought it should be obvious that

$$U_K = S_K C = R_K^{FL} e^{i\alpha} RC = (R_K^{FL})(e^{i\alpha} RC) = R_K^{FL} C^{FL}. \quad (2.36)$$

So the change of approaches is equivalent to the change of the coin operator to $C^{FL} = e^{i\alpha} RC$. However, for the general reflection operator \mathcal{R} from (2.6) where $e^{i\alpha} \neq e^{i\beta}$ the approaches stop being equivalent because of the additional local phases appearing during the reflection.

2.2 Hadamard walk on a finite line and a circle

The case of asymptotic evolution of one particle on a finite line and a circle has already been analyzed in [27]. There the analysis of the case with local reflection operator $\mathcal{R} = \sigma_x$ and a general coin from the $SU(2)$ group has been presented. The parametrization of $SU(2)$ presented in [27] is of the form

$$C = \begin{pmatrix} (e^{i(\alpha+\gamma)} - e^{i(\gamma-\alpha)}) \sin(\beta) \cos(\beta) & e^{-i\alpha} \cos^2(\beta) + e^{i\alpha} \sin^2(\beta) \\ e^{i\alpha} \cos^2(\beta) + e^{-i\alpha} \sin^2(\beta) & (e^{i(\alpha-\gamma)} - e^{-i(\gamma+\alpha)}) \sin(\beta) \cos(\beta) \end{pmatrix}, \quad (2.37)$$

where α, β, γ are real-valued parameters. The Hadamard coin (4.4) corresponds to the choice of parameters

$$\alpha = \pi/4, \quad \beta = \pi/4, \quad \gamma = -\pi/2. \quad (2.38)$$

Only this case, i.e. the Hadamard walk, will be shown here. For the general analysis of percolated one-walker quantum walk in one dimension the reader is referred to [27]. The operator from the coin condition

$$\mathcal{R}H = \frac{1}{\sqrt{2}} \begin{pmatrix} 1 & -1 \\ 1 & 1 \end{pmatrix}, \quad (2.39)$$

has the following eigenvalues and respective orthonormal eigenvectors

$$\begin{aligned} \lambda_+ = \frac{1}{\sqrt{2}}(1 + i) : \quad |+\rangle &= \frac{1}{\sqrt{2}} \begin{pmatrix} i \\ 1 \end{pmatrix} = \frac{1}{\sqrt{2}}(i|L\rangle + |R\rangle), \\ \lambda_- = \frac{1}{\sqrt{2}}(1 - i) : \quad |-\rangle &= \frac{1}{\sqrt{2}} \begin{pmatrix} -i \\ 1 \end{pmatrix} = \frac{1}{\sqrt{2}}(-i|L\rangle + |R\rangle). \end{aligned} \quad (2.40)$$

The shift condition has to be used to build the whole common eigenstates from these local parts. The shift condition (2.33) for common eigenstates $|\phi\rangle$ can be rewritten into the form

$$S_L S_K^\dagger |\phi\rangle = |\phi\rangle. \quad (2.41)$$

For the amplitudes of the common eigenstates this yields

$$\phi_{s,R} = \phi_{s-1,L}, \quad \forall s \in \{1, \dots, N-1\}, \quad (2.42)$$

where $\phi_{s,c} \equiv \langle s, c | \phi \rangle$ are the left and right amplitudes at the individual vertices. One can notice that the condition for $s = 0$ is left out, this is because it depends on the boundary condition, i.e. if the graph is a finite line or a circle. On the circle the condition above holds for $s = 0$ as well, after the identification $N \equiv 0$ is considered. For the finite line the condition simply will not hold, because the walker cannot move further in that direction. For both eigenvalues λ_\pm the eigenspace is one-dimensional, this means that the common eigenstates $|\phi_\pm\rangle$ will have the following shape

$$|\phi_\pm\rangle = \sum_{s=0}^{N-1} \mathbf{a}_s |s, \pm\rangle = \frac{1}{\sqrt{2}} \sum_{s=0}^{N-1} a_s (\pm i |s, L\rangle + |s, R\rangle). \quad (2.43)$$

The shift conditions for the amplitudes $\mathbf{a}^s = (a_{s,L}, a_{s,R})^T = \left(\frac{\pm i}{\sqrt{2}} a_s, \frac{1}{\sqrt{2}} a_s \right)^T$ then read

$$a_{s,R} = a_{s-1,L}, \quad \forall s \in \{1, \dots, N-1\}, \quad (2.44)$$

for the finite line, for the circle this holds also for $s = 0 \equiv N$. Clearly, since in this case $a_{s,R} = a_{s,L} \equiv a_s$, these conditions imply $a_s = a_{s-1}, \forall s \in \{1, \dots, N-1\}$ and also $a_0 = a_{N-1}$ for the circle. So the whole

common eigenstate is in both cases determined by only one parameter and this parameter is in the end determined from normalization. So for the finite line of length N there are two common eigenstates, one for each eigenvalue, of the following form

$$\begin{aligned}\lambda_+ &= \frac{1}{\sqrt{2}}(1 + i) : |\phi_+\rangle = \frac{1}{\sqrt{N}} \sum_{s=0}^{N-1} (-i)^s |s, +\rangle, \\ \lambda_- &= \frac{1}{\sqrt{2}}(1 - i) : |\phi_-\rangle = \frac{1}{\sqrt{N}} \sum_{s=0}^{N-1} (i)^s |s, -\rangle.\end{aligned}\quad (2.45)$$

For the circle there is an additional periodic boundary condition $a_0 = a_{N-1}$, so $(\pm i)^0 = 1 \stackrel{!}{=} (\pm i)^{N-1}$ needs to hold for the given N . It turns out this only holds for $N = 4k, \forall k \in \mathbb{N}$, so for all other circles there are no common eigenstates altogether. This implies that for the finite line and circles of correct lengths the following p-attractors and eigenvalues of the superoperator can be constructed

$$\begin{aligned}\lambda_1 &= \lambda_+ \lambda_+ = i : |\phi_- \rangle \langle \phi_+|, \\ \lambda_2 &= \lambda_+ \lambda_- = 1 : |\phi_- \rangle \langle \phi_-|, |\phi_+ \rangle \langle \phi_+|, \\ \lambda_3 &= \lambda_- \lambda_- = -i : |\phi_+ \rangle \langle \phi_-|.\end{aligned}\quad (2.46)$$

Next part of the analysis is searching for non-p-attractors. It turns out that in many cases the only non-p-attractor is the identity. The aim is now to show that it is truly the case for the Hadamard walk. The construction of the whole attractor is similar to the process of construction of the common eigenstates, just more difficult. Through the modified coin condition (2.27) one can obtain the shapes of individual attractor blocks corresponding to positions $s, t \in \{0, \dots, N-1\}$ for all possible eigenvalues as

$$\begin{aligned}\lambda_1 = i : X_t^s &= a_{s,t} \begin{pmatrix} -1 & i \\ i & 1 \end{pmatrix}, \\ \lambda_2 = 1 : X_t^s &= \begin{pmatrix} b_{s,t} & -c_{s,t} \\ c_{s,t} & b_{s,t} \end{pmatrix}, \\ \lambda_3 = -i : X_t^s &= d_{s,t} \begin{pmatrix} -1 & -i \\ -i & 1 \end{pmatrix},\end{aligned}\quad (2.47)$$

where $a_{s,t}, b_{s,t}, c_{s,t}, d_{s,t} \in \mathbb{C}$ are the coefficients which need to be determined from the shift conditions (2.29). As for the shift conditions, from now on the elements of an attractor X will be denoted in the following way

$$X_{t,d}^{s,c} \equiv \langle s, c | X | t, d \rangle. \quad (2.48)$$

It is maybe also useful to note how does the general attractor block look like in this notation

$$X_t^s = \begin{pmatrix} X_{t,L}^{s,L} & X_{t,R}^{s,L} \\ X_{t,L}^{s,R} & X_{t,R}^{s,R} \end{pmatrix}. \quad (2.49)$$

For the case $s \neq t, \forall s, t \in \{1, \dots, N-1\}$ on the finite line the conditions read

$$X_{t-1,L}^{s-1,L} = X_{t-1,L}^{s,R} = X_{t,R}^{s-1,L} = X_{t,R}^{s,R}. \quad (2.50)$$

For diagonal elements $s = t$ the conditions above split into two parts as

$$\begin{aligned}X_{s-1,L}^{s,R} &= X_{s,R}^{s-1,L}, \\ X_{s-1,L}^{s-1,L} &= X_{s,R}^{s,R}.\end{aligned}\quad (2.51)$$

It is now important to mention how exactly are the p-attractors different from the non-p-attractors. Simply from construction the shift conditions never split, so for a p-attractor Y it holds

$$Y_{t-1,L}^{s-1,L} = Y_{t-1,L}^{s,R} = Y_{t,R}^{s-1,L} = Y_{t,R}^{s,R}, \quad \forall s, t \in \{1, \dots, N-1\}. \quad (2.52)$$

For the circle all of the shift conditions mentioned above for both the general and p-attractors hold also for cases when either s , or t , or both are equal to 0 and the identification $N \equiv 0$ is considered.

In the rest of this section it will be shown how it can be proved that there truly is only one non-p-attractor for the percolated Hadamard walk, and that is the identity I corresponding to the eigenvalue $\lambda_2 = 1$. For both eigenvalues $i, -i$ it is possible to show that any general attractor is a p-attractor. That can be done by proving that the condition (2.50) does not split for the diagonal elements, i.e. holds even for $s = t$. Starting with the eigenvalue $\lambda_1 = i$ the following relations for the coefficients $a_{s,s}, a_{s-1,s}, a_{s,s-1}, a_{s-1,s-1}, \forall s \in \{1, \dots, N-1\}$ can be deduced from the shift conditions (4.8) and (4.12) as

$$\begin{aligned} X_{s-1,L}^{s-1,L} = X_{s,R}^{s,R} &\implies -a_{s-1,s-1} = a_{s,s}, \\ X_{s-1,L}^{s,R} = X_{s,R}^{s-1,L} &\implies ia_{s,s-1} = ia_{s-1,s}, \\ X_{s-1,L}^{s,L} = X_{s,R}^{s,L} &\implies -a_{s,s-1} = ia_{s,s}. \end{aligned} \quad (2.53)$$

From this it is obvious that

$$ia_{s,s-1} = a_{s,s} = -a_{s-1,s-1} \implies X_{s-1,L}^{s-1,L} = X_{s-1,L}^{s,R} = X_{s,R}^{s-1,L} = X_{s,R}^{s,R}, \quad (2.54)$$

so every attractor corresponding to $\lambda_1 = i$ is a p-attractor. Similarly for the eigenvalue $\lambda_3 = -i$ it can be deduced from the general shift conditions that

$$\begin{aligned} X_{s-1,L}^{s-1,L} = X_{s,R}^{s,R} &\implies -d_{s-1,s-1} = d_{s,s}, \\ X_{s-1,L}^{s,R} = X_{s,R}^{s-1,L} &\implies -id_{s,s-1} = -id_{s-1,s}, \\ X_{s-1,L}^{s,L} = X_{s,R}^{s,L} &\implies -d_{s,s-1} = -id_{s,s}, \end{aligned} \quad (2.55)$$

which implies

$$-id_{s,s-1} = d_{s,s} = -d_{s-1,s-1} \implies X_{s-1,L}^{s-1,L} = X_{s-1,L}^{s,R} = X_{s,R}^{s-1,L} = X_{s,R}^{s,R}. \quad (2.56)$$

So once again this shows that every attractor corresponding to the eigenvalue $\lambda_3 = -i$ is a p-attractor.

For the eigenvalue $\lambda_2 = 1$ there is certainly at least one non-p-attractor, the identity I , so it is necessary to proceed in a different way. Here the lower limit for the number of attractors is already determined as the 3 linearly independent that have already been found (two p-attractors and the identity). The upper limit on the dimension of this attractor subspace can be proved to be 3 using the shift conditions. Since upper and lower limit of the dimension are equal, the attractor subspace corresponding to the eigenvalue 1 consists of the three attractors already found. Assuming that the parameters $b_{0,0}, c_{0,0}$ of the first block X_0^0 have already been determined the aim is now to show how far in determining the neighboring blocks one can get from them. Using the shift conditions yields equalities

$$\begin{aligned} X_{0,L}^{0,R} = X_{1,R}^{0,R} &\implies c_{0,0} = b_{0,1}, \\ X_{0,R}^{0,L} = X_{0,R}^{1,R} &\implies -c_{0,0} = b_{1,0}, \\ X_{1,R}^{0,R} = X_{1,R}^{1,L} &\implies b_{0,1} = -c_{1,1}, \\ X_{0,L}^{0,L} = X_{1,R}^{1,R} &\implies b_{1,1} = b_{1,1}. \end{aligned} \quad (2.57)$$

It seems like it is not possible to get any further in the case of a finite line, so the next step is to try fixing some other extra parameter, for example $c_{0,1}$. There through shift conditions one gets

$$X_{1,R}^{0,L} = X_{0,L}^{1,R} \implies -c_{0,1} = c_{1,0}. \quad (2.58)$$

Clearly this has finally determined all of the neighboring blocks X_0^1, X_1^0, X_1^1 . Since the shift conditions from these block can only give the same or larger amount of information about the other blocks, the 3 parameters fixed in the beginning fully determine the whole attractor. So this truly shows that the attractor space corresponding to $\lambda_2 = 1$ is at most three dimensional.

These were the results for the finite line. In case of the circle the coin condition is the same and the shift conditions are the same plus the periodic ones for the ends. This means all of the attractors for the circle are such attractors for the finite line which additionally satisfy the periodic shift conditions. So for the circles of lengths $N = 4k, k \in \mathbb{N}$ the attractors are the same as for the finite line and for others the only attractor is the identity.

Looking back at the resulting asymptotic dynamics one can also notice that none of the attractors is localized. All of the common eigenvectors, for both the case of the finite line and the circle, have non-zero elements on the whole graph. The same then holds for the corresponding p-attractors and of course for the identity as well. This is not exactly a surprise given the dynamics without the percolation. However, the next section will show an interesting effect percolation can have in cases when there is some localized dynamics present originally.

2.3 Lazy walk

One of the interesting properties discovered already about percolated graphs is their positive effect when it comes to transport. It has been shown for example in [7–9] and [29] that adding percolations to the graph can improve its transport properties. Namely it seems like the percolations can sometimes destroy some of the localized eigenstates of the non-percolated evolution meaning the walker has a smaller probability of getting trapped in some part of the system. This section will now show this effect for the simple case of a lazy walk on a line which has been described in [30].

As has been mentioned earlier, lazy walk in the quantum case means adding loops on all of the vertices of the graph. These represent the possibility of the walker to stay in place. The loops are represented by an additional degree of freedom of the local coin spaces. So the local coin spaces are now three-dimensional and their bases are given by the states $\{|L\rangle, |S\rangle, |R\rangle\}$, where $|S\rangle$ is the state representing the loop. The new shift operator is now given as

$$S^{(3)} = S^{(2)} + \sum_{m=0}^{N-1} |m, S\rangle\langle m, S|, \quad (2.59)$$

where the two-state shift operator $S^{(2)}$ is defined either as (2.3) for the finite line, or as (2.4) for the circle. At first, the local coin operator will be specifically chosen as the Grover operator in the above mentioned basis of the local coin space

$$G_3 = \frac{1}{3} \begin{pmatrix} -1 & 2 & 2 \\ 2 & -1 & 2 \\ 2 & 2 & -1 \end{pmatrix}, \quad (2.60)$$

and the special choice of the local reflection operator (2.7) will now be generalized to

$$\mathcal{R}^{(3)} = \begin{pmatrix} 0 & 0 & 1 \\ 0 & 1 & 0 \\ 1 & 0 & 0 \end{pmatrix}. \quad (2.61)$$

The shift operator for a given configuration of edges is now given as

$$S_K^{(3)} = \sum_{(m,m+1) \in K} |m+1, R\rangle\langle m, R| + \sum_{(m-1,m) \in K} |m-1, L\rangle\langle m, L| + \sum_{(m,m+1) \notin K} \mathcal{R}^{(3)} |m, R\rangle\langle m, R| + \sum_{(m-1,m) \notin K} \mathcal{R}^{(3)} |m, L\rangle\langle m, L| + \sum_{m=0}^{N-1} |m, S\rangle\langle m, S|, \quad (2.62)$$

where as one can see the loops are not allowed to be considered broken, only the original underlying graph edges. i.e. the finite line or the circle. The rest of this section will now show an example of how sometimes, but not always, the trapping effect can be eliminated by adding dynamical percolations to the graph.

The trapping effect is associated to the existence of a highly degenerate eigenvalue of the evolution operator whose corresponding eigenvectors are spatially localized. In case of the lazy walk on a line described above the non-percolated evolution has a highly degenerate eigenvalue 1. There exists N corresponding spatially localized linearly independent (but not orthogonal) eigenvectors of the following shape

$$|s_m\rangle = |m\rangle \left(\sqrt{\frac{2}{3}} |L\rangle + \sqrt{\frac{1}{6}} |S\rangle \right) + |m+1\rangle \left(\sqrt{\frac{1}{6}} |S\rangle + \sqrt{\frac{2}{3}} |R\rangle \right), \quad \forall m \in \{0, \dots, N-1\}, \quad (2.63)$$

where the following notation $N \equiv 0$ is used even for the finite line now. For the finite line $|s_N\rangle$ is also an eigenvector because of the choice of the reflection operators at the end of the line. The fact that these truly are eigenvectors can be easily verified by direct calculation. These eigenstates then have the ability to trap parts of the state in some limited spacial region of the underlying graph during the evolution and limit the transport properties of the system.

All common eigenvectors of the percolated walk have to be the eigenvectors of the non-percolated walk as well, the percolation can only destroy eigenstates of the original dynamics. The aim is now to determine whenever the above mentioned eigenstates survive the percolations. That can be done by checking if they satisfy the shift conditions. The general common eigenstate will be of the shape

$$|\phi\rangle = \sum_{m=0}^{N-1} |m\rangle \left(\phi_L^m |L\rangle + \phi_S^m |S\rangle + \phi_R^m |R\rangle \right), \quad (2.64)$$

where the coefficients $\phi_L^m, \phi_S^m, \phi_R^m \in \mathbb{C}$ satisfy the following shift conditions

$$\phi_L^m = \phi_R^{m+1} \quad \forall m \in \{0, \dots, N-2\}. \quad (2.65)$$

For the circle they hold even for $m = N-1$, where $N \equiv 0$. It is however clear that all of the localized eigenstates (2.63) satisfy these conditions and hence do not disappear. So for the Grover coin the trapping effect survives for both the finite line and the circle. This example has shown that the percolations are not a universal solution to eliminating the trapping effect, but the point of this section is to show that they can help at least in some cases. However, as has been mentioned earlier, their positive effect has been found for other graphs with the Grover coin already, for example in [7–9] and [29]. It will now be shown that this effect can be found even for the one-dimensional case. For that it is however necessary to choose a different local coin operator. The group of coins for a lazy walk on a line which exhibits the trapping effects has been found and analyzed in [31] and [32]. In this work only a subclass of the trapping coins whose transport properties were analyzed in detail in [30] will be taken into account.

So the new generalized local coin operator will now be taken as

$$G^{\rho,\alpha} = \begin{pmatrix} -\rho^2 & \rho \sqrt{2(1-\rho^2)} & e^{-i\alpha}(1-\rho^2) \\ \rho \sqrt{2(1-\rho^2)} & 2\rho^2 - 1 & e^{-i\alpha}\rho \sqrt{2(1-\rho^2)} \\ e^{i\alpha}(1-\rho^2) & e^{i\alpha}\rho \sqrt{2(1-\rho^2)} & -\rho^2 \end{pmatrix}, \quad (2.66)$$

where $\alpha \in [0, 2\pi]$ and $\rho \in [0, 1]$. The Grover operator is included in this class of coins under the choice of parameters $\alpha = 0$ and $\rho = \sqrt{2/3}$. For this class of coins there again exist the N spatially localized eigenvectors of the non-percolated walk corresponding to the eigenvalue 1. They are of the shape

$$|s_m^{\rho,\alpha}\rangle = |m\rangle \left(\sqrt{1-\rho^2} |L\rangle + \frac{\rho}{\sqrt{2}} |S\rangle \right) + |m+1\rangle \left(\frac{\rho}{\sqrt{2}} |S\rangle + e^{i\alpha} \sqrt{2(1-\rho^2)} |R\rangle \right), \quad \forall m \in \{0, \dots, N-1\}. \quad (2.67)$$

Looking at the shift conditions (2.64) it is clear that these localized eigenvectors will disappear for the percolated walk for all cases when $\alpha \neq 0$. So despite the intuition, random breaking of edges can truly in some cases improve transport properties of the system.

Chapter 3

Two-particle quantum walks

In this chapter the concept of multi-particle quantum walks will be explained and some of the previous work concerning the topic of two-particle quantum walks will be summarized. The chapter will also introduce the formalism for the last chapter of this work which then discusses the new results obtained on the topic of percolated two-particle walks.

Here the quantum walk of two particles on the same graph will be defined as a quantum walk on a Hilbert space

$$\mathcal{H} = \mathcal{H}^{(1)} \otimes \mathcal{H}^{(1)} = (\mathcal{H}_p \otimes \mathcal{H}_c) \otimes (\mathcal{H}_p \otimes \mathcal{H}_c), \quad (3.1)$$

where $\mathcal{H}^{(1)}$ is the Hilbert space of one particle. The evolution operator without interaction is defined as

$$U = U_1^{(1)} \otimes U_2^{(1)}, \quad (3.2)$$

where $U_1^{(1)}$ and $U_2^{(1)}$ are one-particle evolution operators. The one-particle operators $U_1^{(1)}$ and $U_2^{(1)}$ are again of the structure

$$U_i^{(1)} = S_i^{(1)} C_i^{(1)}, \quad \forall i \in \{1, 2\}, \quad (3.3)$$

where $S_i^{(1)}$ and $C_i^{(1)}$ are respectively the one-walker shift and coin operators for $i \in \{1, 2\}$. In general the one-walker evolution operators can be different, but since both of the particles walk on the same graph one usually considers the same walks. So then $U^{(1)} = U_1^{(1)} = U_2^{(1)}$ and the total evolution operator is equal to

$$U = U^{(1)} \otimes U^{(1)}. \quad (3.4)$$

With more walkers present there is also the question of their indistinguishability. In cases where one considers the walkers being distinguishable, the Hilbert space is defined as above and everything works just as it is. However, for the cases of indistinguishable particles some adjustments are needed. Briefly recapitulating, the types of quantum indistinguishable particles are bosons and fermions. Bosonic particles have allowed states only in the totally symmetrical subspace of the Hilbert space, while fermionic particles are allowed to have only totally antisymmetrical states from the Hilbert space. The total symmetry, or antisymmetry of the state is meant in the context of exchanging labels of the individual particles. So for N identical particles on the original Hilbert space \mathcal{H} the bosons exist on the (closed) subspace $\mathcal{S}_N \mathcal{H}$, where \mathcal{S}_N is a projector defined as

$$\mathcal{S}_N = \frac{1}{N!} \sum_{\sigma \in \mathfrak{S}_N} U_\sigma. \quad (3.5)$$

Here the unitary operators U_σ correspond to the permutations σ of the particles from the set of all possible permutations of N particles \mathfrak{S}_N . Similarly for N fermions the (closed) subspace of allowed

states is given as $\mathcal{A}_N \mathcal{H}$, where the projector \mathcal{A}_N is similarly defined as

$$\mathcal{A}_N = \frac{1}{N!} \sum_{\sigma \in \mathfrak{S}_N} \text{sgn}(\sigma) U_\sigma. \quad (3.6)$$

Here $\text{sgn}(\sigma)$ denotes the sign of the permutation σ . The time evolution of the symmetrical, or the antisymmetrical initial state then stays in the given subspace, because the evolution operator is invariant towards the exchange of the two particles. So for the case of two walkers the projectors are of the following shape

$$\mathcal{S}_2 = \frac{1}{2} (I + W), \quad \mathcal{A}_2 = \frac{1}{2} (I - W), \quad (3.7)$$

where W denotes an operator which exchanges the two particles. For some pure state $|\psi\rangle \in \mathcal{H}$ the symmetrical and antisymmetrical projections are clearly given as $\mathcal{S}_2 |\psi\rangle$ and $\mathcal{A}_2 |\psi\rangle$. For a general density matrix $\rho \in \mathcal{B}(\mathcal{H})$ the corresponding bosonic and fermionic density matrices are then given as $\mathcal{S}_2 \rho \mathcal{S}_2$ and $\mathcal{A}_2 \rho \mathcal{A}_2$.

There are not many results in the literature for the multi-particle quantum walks mainly due to the complications caused by the increasing dimensionality of the problem. The case of two-particle discrete-time quantum walks on the line have been considered for example in [33] and [34]. The summary of their results will now be briefly presented. It is quite obvious from the above definition of the evolution operator (3.2) that non-interacting walk cannot generate entanglement. So for a separable initial state of the two walkers the evolution will stay separable. Formally, if the initial state of the walkers is of the shape $|\psi_0\rangle = |\psi_0^{(1)}\rangle \otimes |\psi_0^{(2)}\rangle$ the application of the evolution operator will generate the final state after $t \in \mathbb{N}$ steps of the shape

$$|\psi_t\rangle = (U^{(1)})^t |\psi_0^{(1)}\rangle \otimes (U^{(2)})^t |\psi_0^{(2)}\rangle \equiv |\psi_t^{(1)}\rangle \otimes |\psi_t^{(2)}\rangle. \quad (3.8)$$

So the two-walker evolution is fully determined by the one-particle evolution and the probability distribution for the first and second particle being on positions m and n respectively after $t \in \mathbb{N}$ steps of the walk is given as

$$P_{12}(m, n, t) = P_1(m, t) \times P_2(n, t). \quad (3.9)$$

Here index 12 denotes the two-particle probability distribution and indices 1 and 2 denote the one-particle distributions of the first and second particle. In general, the probability distributions for the final one-particle states $|\psi_t^{(k)}\rangle$ for $k \in \{1, 2\}$ and the final two-particle state $|\psi_t\rangle$ are defined as

$$\begin{aligned} P_k(m, t) &= \sum_{c \in \{L, R\}} |\langle \psi_t^{(k)} | m, c \rangle|^2, \quad \forall k \in \{1, 2\}, \\ P_{12}(m, n, t) &= \sum_{c, d \in \{L, R\}} |\langle \psi_t | m, c, n, d \rangle|^2. \end{aligned} \quad (3.10)$$

In the case of separable initial state and non-interacting evolution operator the walk can be fully described by the results from Chapter 1. However, for the case of entangled initial state the situation becomes more complicated. This case has been the main focus of [33] for the Hadamard walk on a line of two distinguishable walkers and their results will now be shortly summarized. For the entangled case it is worth to start working with the density matrices of the system. Denoting the final density matrices ρ_t and $\rho_t^{(k)}$, $\forall k \in \{1, 2\}$ for the two-particle and one-particle case respectively, the formulas (3.10) can be

rewritten as

$$\begin{aligned}
P_k(m, t) &= \sum_{c \in \{L, R\}} \left| \langle m, c | \rho_t^{(k)} | m, c \rangle \right|^2, \quad \forall k \in \{1, 2\}, \\
P_{12}(m, n, t) &= \sum_{c, d \in \{L, R\}} |\langle m, c, n, d | \rho_t | m, c, n, d \rangle|^2.
\end{aligned} \tag{3.11}$$

The one-particle states $\rho_t^{(1)}$ and $\rho_t^{(2)}$ are described by the reduced density matrices, i.e. $\rho_t^{(1)} = \text{Tr}_2(\rho_t)$ and $\rho_t^{(2)} = \text{Tr}_1(\rho_t)$. The traces Tr_1 and Tr_2 are the partial traces over the spaces of the first and the second particle respectively. In [33] the cases of three initial states spatially localized at the origin of the line were considered

$$\begin{aligned}
|\Psi_{\pm}\rangle &= \frac{1}{\sqrt{2}} (|0, L, 0, R\rangle \pm |0, R, 0, L\rangle), \\
|\Psi_S\rangle &= |0, L, 0, R\rangle.
\end{aligned} \tag{3.12}$$

The state $|\Psi_S\rangle$ is clearly separable, however the other two are entangled, more specifically entangled in their coin degrees of freedom. The coins are in two of the four of the maximally entangled two-qubit states called the Bell states. For these states they then proceeded to both numerically and analytically investigate several properties of the system with respect to the entanglement of the initial state. The first quality is of course the probability distribution $P_{12}(m, n, t)$ for the entangled initial states. It turns out that for the above mentioned entangled initial states the probability distribution contains also some interference terms next to the one-particle probabilities. Because of this some joint, rather than one-particle, properties were investigated, for example the mean value of observable $\langle \hat{x}_1 \hat{x}_2 \rangle$. Here the operators \hat{x}_1 and \hat{x}_2 are the operators of position of the first and second particle respectively.

This expectation value is interesting because together with the knowledge of $\langle \hat{x}_1 \rangle$ and $\langle \hat{x}_2 \rangle$ for the one-particle walk on a line one can calculate the correlation function $C_{12} = \langle \hat{x}_1 \hat{x}_2 \rangle - \langle \hat{x}_1 \rangle \langle \hat{x}_2 \rangle$. For the separable initial state one, not very surprisingly, gets the following result

$$\langle \hat{x}_1 \hat{x}_2 \rangle^S = \langle \hat{x}_1 \rangle \langle \hat{x}_2 \rangle = -\langle \hat{x}_1 \rangle^2. \tag{3.13}$$

For the entangled states there is an extra term and the resulting mean value is then of shape

$$\langle \hat{x}_1 \hat{x}_2 \rangle^{\pm} = -\langle \hat{x}_1 \rangle^2 \pm \|I_{\downarrow\uparrow}\|^2, \tag{3.14}$$

where for the definition of the interference term $I_{\downarrow\uparrow}$ see eq. (23) in [33]. Analysis shows that after $t \in \mathbb{N}$ steps of the evolution these mean values exhibit the following behavior

$$\langle \hat{x}_1 \hat{x}_2 \rangle^{S,-} \propto t^2, \quad \langle \hat{x}_1 \hat{x}_2 \rangle^+ \propto t. \tag{3.15}$$

It is also obvious that $\langle \hat{x}_1 \hat{x}_2 \rangle^- < \langle \hat{x}_1 \hat{x}_2 \rangle^S$ which actually holds for any separable initial state. This is an example of the fact, that entanglement can provide qualities which cannot be reached with separable states.

The average squared distance $\langle \hat{\Delta}_{12}^2 \rangle \equiv \langle (\hat{x}_1 - \hat{x}_2)^2 \rangle$ scales quadratically with t and the linear distance $\langle \hat{\Delta}_{12} \rangle \equiv \langle |\hat{x}_1 - \hat{x}_2| \rangle$ linearly with t . From the numerical results the particles with the '+' initial state tend to stay closer together while the ones with '-' further away. Considering the fact that these initial states can be taken as initial states for bosonic and fermionic particles in the indistinguishable case, it is not such a surprising result. For the probabilities of finding at least one particle on a given position m after t steps of the evolution there are similar differences. While for the '-' initial state the probability is always

greater than for the separable initial state, for the '+' initial state it is always smaller. This is an example how certain properties of the walk can be enhanced or suppressed purely by entanglement and also that certain properties are unattainable without entanglement completely.

Another typical quality of interest for the case of more walkers is the probability of them meeting on the same position. The probability of both walkers being on a position m after t steps of the evolution is given as

$$M(m, t) = P_{12}(m, m, t). \quad (3.16)$$

The total probability of meeting after t steps of the walk is then

$$M(t) = \sum_m M(m, t). \quad (3.17)$$

The overall probability that the walkers meet at least once during the first T steps of the walk can then be expressed as

$$\overline{M}(T) = 1 - \prod_{t=1}^T (1 - M(t)). \quad (3.18)$$

This meeting problem was investigated in [34] for the non-interacting Hadamard walk of both two distinguishable and indistinguishable particles. The results were also compared to the classical meeting problem.

The initial states of the walkers considered in [34] are always localized with one walker being at the origin of the line and the second on the position $2d$ for $d \in \mathbb{N} \cup \{0\}$. The dependence of the meeting probabilities is also analyzed for different distances d . Their initial distance truly must be even, otherwise the walkers will never meet because of the walk being bipartite. The initial coin states of the distinguishable particles are first taken separable as $|L\rangle$ for one walker and $|R\rangle$ for the other, or both having symmetric initial conditions provided by coin state $1/\sqrt{2}(|L\rangle + i|R\rangle)$. So for the first walker being biased to the left and the second to the right the walkers are expected to move away from each other. If the situation would be reversed they should have the tendency to move towards each other. For the symmetrical initial conditions the probability distribution is expected to be symmetrical and unbiased.

In general $M(t)$ in the quantum case decays slower than in the classical case while reaching the peak sooner than in the classical case. So while at the beginning of the walk the quantum meeting probabilities are higher than the classical ones, for large number of steps the classical case becomes dominant. Not surprisingly the largest meeting probability can be obtained via the initial state where the walkers are biased towards each other, while the smallest one is for the case when they are biased initially facing away from each other. As for the overall meeting probability $\overline{M}(T)$, investigated as a function of the initial distance, while starting as the highest the classical case also drops the fastest with the increasing d compared to the quantum cases. Out of the quantum cases the particles initially directed towards each other exhibit the slowest decay of $\overline{M}(T)$ with d . The next is then the symmetrical case and the fastest decay out of the quantum cases has the initial state with particles directed from each other. As for the behavior for large T , the quantum cases converge to one faster than the classical case.

Next, the effect of entanglement on the distinguishable particles was studied. Here the spatial part of the initial state is still the same, the walkers are $2d$ places from each other, but the coin states is taken as one of the Bell states

$$\begin{aligned} |\psi_{\pm}\rangle &= \frac{1}{\sqrt{2}} (|LR\rangle \pm |RL\rangle), \\ |\phi_{\pm}\rangle &= \frac{1}{\sqrt{2}} (|RR\rangle \pm |LL\rangle). \end{aligned} \quad (3.19)$$

To see the effect of interference the meeting probabilities $M(t)$ were compared to the meeting probabilities of the symmetrical case of distinguishable particles. It can again be seen that the effect of entanglement can be both positive and negative. Also the effects for $|\psi_{-}\rangle$ are the opposite to the ones of $|\phi_{+}\rangle$ and for $|\psi_{+}\rangle$ they are the opposite to the ones of $|\phi_{-}\rangle$. The peak values are at similar points of the evolution, however the peak value is much bigger for $|\psi_{-}\rangle$ (so also much smaller for $|\phi_{+}\rangle$). The case of $|\psi_{-}\rangle$ also decays much faster on the long time scale. So the initial entanglement of the walkers affects both the maximum meeting probability and also the long time scale behavior.

At last [34] comments on the effect of indistinguishability of the walkers. An example initial coin state where one particle starts in $|L\rangle$ and one in $|R\rangle$ shows meeting probability greater for bosons and smaller for fermions compared to distinguishable particles. For fermions the explanation is the exclusion principle which simply works against the meeting probability.

Another possible quality of interest can be the probability of finding both of the walkers on the same side of the line as it was studied in [35]. The probability of finding both walkers on the same side of the line in $t \in \mathbb{N}$ step of the walk is for both walkers starting at the origin defined as

$$P_s(t) = \sum_{m,n=-t}^0 P_{12}(m,n,t) + \sum_{m,n=1}^t P_{12}(m,n,t), \quad (3.20)$$

for distinguishable particles and as

$$P_s(t) = \sum_{n=-t}^0 \left(\sum_{m=n}^0 P_{12}(m,n,t) \right) + \sum_{n=1}^t \left(\sum_{m=n}^t P_{12}(m,n,t) \right), \quad (3.21)$$

for the indistinguishable case. So the initial state of both walkers is localized in the origin, but what about the coin. Lets first take a look at the separable initial condition. General initial single-particle coin state can be rewritten in the Hadamard basis, i.e. the eigenstates of the Hadamard coin,

$$|\chi^{\pm}\rangle = \frac{\sqrt{2 \pm \sqrt{2}}}{2} |L\rangle \pm \frac{\sqrt{2 \mp \sqrt{2}}}{2} |R\rangle, \quad (3.22)$$

so that for both particles

$$|\psi_i\rangle = h_i^+ |\chi^+\rangle + h_i^- |\chi^-\rangle, \quad \forall i \in \{1, 2\}, \quad (3.23)$$

where the coefficients $h_i^{\pm} \in \mathbb{C}$ satisfy the normalization condition. The probability of finding particles on the same side of the line in the asymptotic limit for the separable initial state is then equal to

$$P_s^{(sep)} = \frac{1}{4} [2 + (2|h_1^+|^2 - 1)(2|h_2^+|^2 - 1)]. \quad (3.24)$$

The minimum obtainable probability is 1/4 and the maximum 3/4.

As for the entangled initial coin state, one can again use the Hadamard basis to write down the general two-particle coin state as

$$|\psi_C\rangle = \sum_{c,d=\pm} h_{(cd)} |\chi^c\rangle |\chi^d\rangle, \quad (3.25)$$

where the coefficients $h_{(cd)} \in \mathbb{C}$ again satisfy the normalization condition. The asymptotic probability of the particles being on the same side of the line is then given as

$$P_s^{(ent)} = \frac{1}{4} \left[1 + 2 \left(|h_{(++)}|^2 + |h_{(--)}|^2 \right) \right]. \quad (3.26)$$

The minimum and maximal obtainable probabilities are again 1/4 and 3/4. For more details and derivations of these formulas see [35].

3.1 Introducing interaction

When talking about multi-particle quantum evolution in general, the possible interaction of the particles and its effects are naturally of interest. In case of quantum walks, especially the discrete-time version, the question of how to introduce interaction is also non-trivial. The continuous-time case directly works with the Hamiltonian to which it is easy to add some interaction part. For the discrete time it is necessary to somehow directly introduce the interaction in the evolution operator which then makes the total evolution operator U non-separable (i.e. it cannot be written in the form (3.2) anymore). Generally, it is done by changing the coin operator in case the walkers are in the same position as for example in [35–37] and [38]. The three possibilities mentioned in these works will now be introduced in this section.

In [37] and [36] two possible interactions called the I -interaction and the π -interaction are discussed. The I -interaction is basically a change of the local (one-particle) coin operator to $-I^{(1)}$, so the negative one-particle identity. So for the Hadamard walk the two-particle local coin operator becomes

$$C^{(2)} = \begin{cases} H \otimes H & \dots x \neq y, \\ -I^{(1)} \otimes -I^{(1)} = I & \dots x = y, \end{cases}$$

for x, y being the positions of the first and second walker. According to the authors of this proposed interaction in [37] it is inspired by the use of quantum oracle in search algorithms. The π -interaction adds a phase $e^{i\pi}$ to the coin operator if the particles are on the same vertex. For the Hadamard walk this means

$$C^{(2)} = \begin{cases} H \otimes H & \dots x \neq y, \\ e^{i\pi} H \otimes H & \dots x = y, \end{cases}$$

where x, y are again the positions of the first and second walker.

In [37] the effect of these two kinds of interaction on one-particle distribution was studied for several different initial conditions localized in the origin of the line. The initial coin states considered were the Bell states (3.19) and one separable symmetrical state. In their numerical results it can be seen that both interaction generate spatial correlations between two particles even for separable initial states. Next, the effect on entanglement of the two particles was investigated for the same initial states. The von Neumann entropy S of the reduced density matrix of either subsystem, ρ_1 or ρ_2 , was used as a measure of entanglement E of these pure initial states $|\psi\rangle$. More specifically S is defined as

$$E(|\psi\rangle) := S(\rho_1) = S(\rho_2) = -\text{Tr}[\rho_1 \log_2 \rho_1] = -\sum_i \lambda_i \log_2 \lambda_i, \quad (3.27)$$

where λ_i are the eigenvalues of the reduced density matrices. As a reminder, the reduced density matrices of the subsystems are defined as

$$\rho_1 = \text{Tr}_2[\rho], \quad \rho_2 = \text{Tr}_1[\rho], \quad (3.28)$$

where ρ is the density matrix of the whole system and Tr_1 and Tr_2 denote the partial traces over the spaces of the first and second particle respectively. The numerical simulations in [36] were done for the Hadamard walk on both the infinite line and the cycle. They show that both types of interaction are capable of generating entanglement even for initially separable states. When comparing the entanglement values for the chosen initial states the π -interaction seems to be generating more entanglement than the I -interaction. This can be connected to the fact that while the π -interaction seemed to enhance the probability of the two walkers being on the same position, the I -interaction created more spatially separated states. This would mean that for the π -interaction walkers have larger possibility to interact than for the I -interaction. In [37] the two-particle walk on general graphs with Grover coin operator and π -interaction

was used to create a procedure for testing graph isomorphism based on the final probability distribution after a certain number of steps. Two undirected graphs are isomorphic if by some permutation of vertices labels one can get the same graphs. What makes the graph isomorphism problem interesting is that it is generally not known to be solvable in polynomial time, nor to be NP-complete. The proposed protocol was able to distinguish some, but unfortunately not all isomorphic undirected graphs. It was however able to distinguish all non-isomorphic graphs tested and worked completely on a certain specific families of graphs.

In [36] the same kinds of interactions were then used to create a quantum Hash scheme. By Hash function is meant any function which maps data of arbitrary size to some values of fixed size. The proposed scheme takes arbitrarily large bit-strings and produces probability distributions of the two-walker one-dimensional quantum walk. The two interactions are used to create two different evolution operators U_0 and U_1 . The system is taken in some chosen initial state and, depending on whenever the next bit in the string is 0 or 1, one of the evolution operators is applied. After applying the unitary operators of the whole message the systems' probability distribution is taken as the result. The main problem however lies in the existence of conflicts, i.e. a lot of initial states produce the same final probability distributions for different input strings.

As for the [38], an interesting work was done regarding the analysis of a generalized π -interaction. They were looking for bound (molecular) states of the two walkers caused by the defined on-site interaction, an analogy of the continuous time molecular states. Molecular bound states of two atoms are in [38] defined by the following dynamical condition: the distance between the atoms remains the same for all times, but the center of mass degree of freedom can exhibit quantum spreading of wave packets. The detailed analysis of the formation and behavior of these molecular states was done in [38] just for the fermionic case. However, an argument about existence of this phenomenon also for the bosonic and distinguishable case was presented there as well, the fermionic case is just apparently slightly easier to solve. The free walk itself is considered to be the Hadamard walk presented above, however it was proved that the effect can be exhibited in much broader context of walks. The interaction is then considered as a change of phase upon meeting as in (3.27), just that the phase now can be some general $g \in \mathbb{R}$, not just $g = \pi$ which turns out to be the maximal interaction case. Numerical simulation presented, and even the ones from the other papers about interacting walks mentioned in this chapter, show a very distinct centering of the probability distribution around the diagonal elements. Also the width around the diagonal is constant in time, which exactly signals the presence of bound states. Another sign of appearance of these states can be found in the spectrum of the evolution operator. It turns out that the interaction brings a new set of eigenvalues where there was a spectral gap for the free walk case. These eigenvalues have been explicitly found in [38] together with the corresponding eigenstates. Example of these new eigenvalues can be seen on Fig. 3.1, where the spectrum of the Fourier block for the circle of length $N = 12$ is shown.

One additional interesting thing about the free walk unitary operator, i.e. without interaction, is that Fourier transform can again be of use. In the momentum representation the evolution operator can be diagonalized separately for each value of the conserved total quasi-momentum $p = p_1 + p_2$ where p_1 and p_2 are the quasi-momenta of individual walkers. One is then left with wave functions depending on the relative momentum $k = (p_1 - p_2)/2$. Using this, an explicit prescription for the bound eigenvalues $e^{i\omega}$ can be found as well as the prescription for the corresponding eigenstates in the momentum space. As for the formation of the molecules in a specific walk, it is clear that initial states where the walkers are localized produce higher probabilities of finding the walkers in a molecular state. This is because of a larger overlap with the above mentioned bounded eigenstates.

One last interesting note about the bound molecular states is whenever this quasi-particle actually performs a quantum walk on the line or a circle as well. It turns out that it indeed does because the effec-

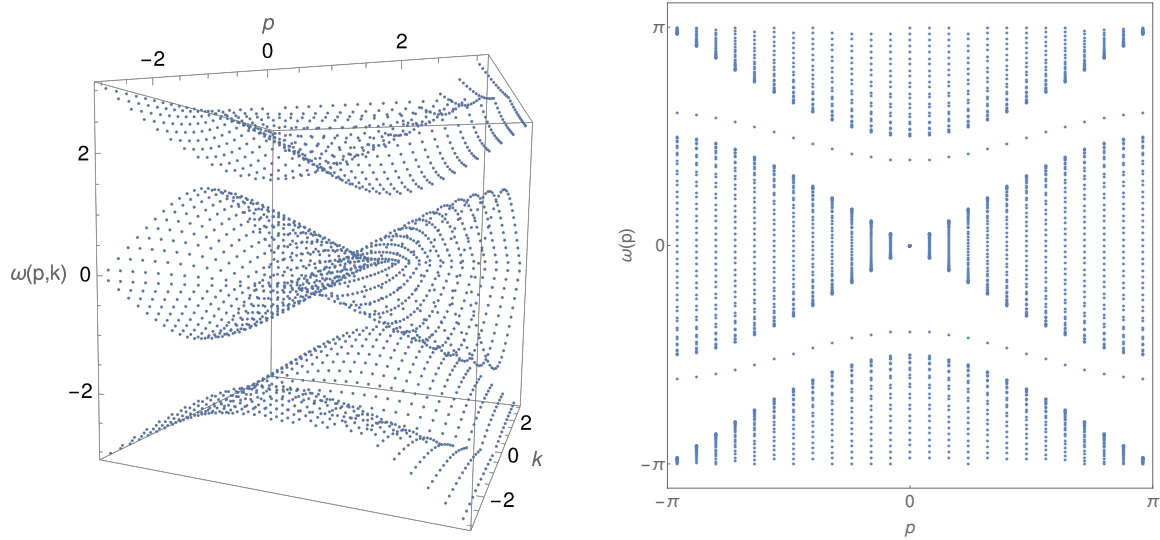


Figure 3.1: Spectrum of the interacting two-particle walk operator on a circle of length $N = 12$. On the left there is the non-interacting case, where the relative momentum is also conserved (represented as a third direction, orthogonal to the paper plane). For the cases of large circles the points will fill the surfaces they are starting to form. On the right panel is the maximally interacting case, where the bands are equal to the projection of the left-panel figure onto the (p, ω) -plane. The additional simple eigenvalues in the band gap are caused by the interaction.

tive evolution operator can be decomposed into an continuing shift operator (1.18) and a coin operator of a specific shape determined by the strength of the interaction g .

There is also an option to change the local two-walker coin operator upon the two walkers meeting in such a way, that it will not be separable anymore. Such a case has been presented in [35] as a δ_x interaction, where for the Hadamard walk on the line they chose

$$C_\delta = \begin{pmatrix} 1 & 1 & 1 & 1 \\ 1 & -1 & -1 & 1 \\ -1 & 1 & -1 & 1 \\ -1 & -1 & 1 & 1 \end{pmatrix}. \quad (3.29)$$

So the local coin operator would now be

$$C^{(2)} = \begin{cases} H \otimes H & \dots x \neq y, \\ C_\delta & \dots x = y, \end{cases}$$

where x, y once again denote the positions of the first and the second walker. In [35] numerical simulation showed that this kind of interaction can help to increase the upper limit for the probability of finding both particles on the same side of the line. This simulation also showed that overall this kind of interaction also tends to increase the diagonal elements of the probability distribution as do the previous ones.

3.2 Percolated quantum walks

There is in general even less literature concerning the percolations in multi-particle quantum walks. This is probably mainly because of the increasing dimensionality of the problem and consequently also of the computational power necessary even for the numerical simulations alone.

The two works directly relevant for this work, i.e. about the dynamical percolations in discrete-time two-particle quantum walks, are [39] and [40]. Both of them contain analysis of numerical simulations of the two-particle discrete-time quantum walks on a line for the cases of both static and dynamical percolations. Just as a reminder, by static percolation one means that at the beginning the configuration of edges is randomly chosen and stays like that for the whole duration of the walk. The first work [39] analyses the walk without any interaction present while [40] includes the π -interaction between the walkers introduced in the previous section. Both of them study the cases of bosons, fermions and classical indistinguishable walkers starting from the origin of the line. The shift operator for the individual walkers is the same as has been introduced in the previous chapter for the percolated walk on the line, i.e. the same as will be used in the next chapter. The coin used is also in both cases the Hadamard coin. Both works study the dependence of certain chosen qualities of the walk on the percolation parameter p , so on the probability of the individual edges being broken. The investigated qualities and the results of these two works will be now shortly summarized.

Talking about identical particles it would now be good to explain what is meant by classical indistinguishable particles in the quantum realm. In the two works mentioned these particles are modeled in the following way. The initial state is taken as a separable state $|\psi_0\rangle = |\psi_1\rangle \otimes |\psi_2\rangle$ and the final measurement stage is modified so that the final probabilities are symmetric under particle exchange. That is done by adding the following projectors to the measurement

$$\Pi_{ij} = \Pi_{ji} = \frac{1}{2}[(|i\rangle\langle i| \otimes I_C) \otimes (|j\rangle\langle j| \otimes I_C) + (|j\rangle\langle j| \otimes I_C) \otimes (|i\rangle\langle i| \otimes I_C)], \quad (3.30)$$

where I_C is an identity on a single-particle local coin space and $|i\rangle, |j\rangle$ are the states in the position spaces of the individual walkers. The final symmetric probabilities $P_2(i, j, t)$ of particles being measured in positions $|i\rangle$ and $|j\rangle$ after $t \in \mathbb{N}$ steps under the evolution operator U are given as

$$P_{12}(i, j, t) = \text{Tr} \left[\Pi_{ij} U^t |\psi_0\rangle\langle\psi_0| (U^\dagger)^t \right]. \quad (3.31)$$

The initial states considered were in both cases spatially localized at the origin, i.e. both walkers start in the middle of the line. The coin states of individual particles considered were then taken as

$$|\varphi_\pm\rangle = \frac{1}{\sqrt{2}} (\pm i |L\rangle + |R\rangle), \quad (3.32)$$

to avoid asymmetrical spreading of the walk. However, after the symmetrization for the three different types of identical walkers one gets the initial states as

$$\begin{aligned} |\Phi_+\rangle &= \frac{1}{\sqrt{2}} (|0, L, 0, L\rangle + |0, R, 0, R\rangle), \\ |\Phi_-\rangle &= \frac{1}{\sqrt{2}} (|0, R, 0, L\rangle - |0, L, 0, R\rangle), \\ |\Psi_S\rangle &= |\varphi_+\rangle \otimes |\varphi_-\rangle, \end{aligned} \quad (3.33)$$

for bosons, fermions and classical indistinguishable particles in this order.

In [39] two global quantities were investigated for different probabilities of the single edge being broken p on $t = 15$ steps of the walk. First one is the average distance between the walkers formally defined as

$$D(t) = \sum_{m,n} |m - n| P_{12}(m, n, t), \quad (3.34)$$

and the second one is the meeting probability, i.e. the probability of the two walkers being in the same place, defined as

$$M(t) = \sum_m P_{12}(m, m, t). \quad (3.35)$$

Not surprisingly the average distance tends to be smaller for static percolations while the meeting probability tends to be larger for static percolations. That can be understood as a result of the particles having larger probability of getting stuck near the origin in this case. In both regimes of noisy environment there is a significant difference in the values of both of the qualities based on the chosen quantum particle statistic. The multi-particle effects of bosons and fermions clearly survive the noisy regimes. Last studied quantity in this work was the probability of finding both of the walkers in their initial starting position $P_2(0, 0, t)$. On simulations of $t = 7$ steps of the walk it was shown that this quantity can be used to estimate the percolation parameter p of the environment more efficiently than by using a single walker. Another interesting thing from the results of this work is the fact that the two-particle walk cannot spread faster than the single-particle one. In fact it can be shown that for every two-particle walk there is always a faster single-particle one. Also, the spreading in the dynamical percolation regimes is of a diffusive character while normally it is ballistic and in the static case the wavefunction has a tendency to have localized peaks.

As for [40], the interaction considered is the π -interaction defined as (3.27) and the simulations are done with the same initial states as in [39], but this time for $t = 20$ steps of the walks. While without the percolation the interaction seems to reduce the effect of the different indistinguishable statistics, in case of percolations being present the situation is different. While the interaction in general causes localization on the diagonal line of the probability distribution (see also the previous section), for dynamical regime it becomes more spread out and less localized in the center. However, there are still differences between different types of indistinguishable particles, so clearly the interaction of inter-particle correlations with the noisy environment is of importance. As for the average distance and the meeting probability of the two walkers, a major difference can be found in both cases when compared to the case without interaction. Without interaction the average distance of fermions is always higher than that of bosons and the meeting probability has the opposite trend. With interaction there seem to be values of percolation probabilities p such that these relationships switch. So for both percolation regimes there are values of p from which the above mentioned relationships become the opposite. Clearly this behavior is induced by the combination of interaction and noisy environment.

Chapter 4

Asymptotic evolution of percolated two-particle walk

Last chapter of this work will show the results and proofs obtained for the asymptotic evolution of the two-walker discrete time percolated quantum walk on a finite line and a circle.

The Hilbert space and evolution of the non-percolated two-particle walk in one dimension are defined as has been described in the previous chapter. The two-particle superoperator describing the percolated quantum walk is now given as

$$\Phi(\rho) = \sum_{K \subset E} p_i (U_K \otimes U_K) \rho (U_K^\dagger \otimes U_K^\dagger), \quad (4.1)$$

where ρ is the two-particle density matrix and U_K are the one-particle evolution operators corresponding to the graph configurations K .

With the same procedure as for the single-particle quantum walk, one arrives at the condition for two-particle attractors X and their corresponding eigenvalues $\lambda \in \mathbb{C}$ of the form

$$(U_K \otimes U_K)X(U_K \otimes U_K)^\dagger = \lambda X, \quad \forall K \subset E. \quad (4.2)$$

This condition can be again split into the shift and coin condition as will be done later. The focus will be once more on the special case when the local reflection operator is chosen as

$$\mathcal{R} = \begin{pmatrix} 0 & 1 \\ 1 & 0 \end{pmatrix} = \sigma_x. \quad (4.3)$$

In addition to that the case of the Hadamard coin as a one-particle local coin operator at every position will be considered

$$C = H = \frac{1}{\sqrt{2}} \begin{pmatrix} 1 & 1 \\ 1 & -1 \end{pmatrix}, \quad (4.4)$$

which means, that the global one-particle coin operator is again

$$C = \bigotimes_{s=0}^{N-1} H. \quad (4.5)$$

4.1 Shift conditions

With similar steps as in the case of one walker, one gets the shift condition for two walkers as

$$(S_L S_K^\dagger \otimes S_L S_K^\dagger)X(S_K S_L^\dagger \otimes S_K S_L^\dagger) = X \quad \forall L, K \subset E. \quad (4.6)$$

The elements of the general attractor X will be again denoted as

$$X_{u,E,v,F}^{s,C,t,D} \equiv \langle s, C, t, D | X | u, E, v, F \rangle, \quad (4.7)$$

where $s, t, u, v \in V$ and C, D, E, F are the corresponding coin states. The whole attractor block for the first walker on vertices s, u and the second walker on vertices t, v will then be denoted as $X_{(u,v)}^{(s,t)}$.

The next step it then to write down the shift conditions for these elements. If none of the position indices are the same, the conditions are

$$\begin{aligned} X_{u,R,v,R}^{s,R,t,R} &= X_{u,R,v,R}^{s-1,L,t,R} = X_{u-1,L,v-1,L}^{s,R,t-1,L} = X_{u,R,v,R}^{s,R,t-1,L} = X_{u-1,L,v-1,L}^{s-1,L,t,R} = \\ &= X_{u-1,L,v,R}^{s,R,t,R} = X_{u,R,v-1,L}^{s-1,L,t-1,L} = X_{u,R,v-1,L}^{s,R,t,R} = X_{u-1,L,v,R}^{s-1,L,t-1,L} = \\ &= X_{u,R,v,R}^{s-1,L,t-1,L} = X_{u-1,L,v-1,L}^{s,R,t,R} = X_{u-1,L,v,R}^{s-1,L,t,R} = X_{u,R,v-1,L}^{s,R,t-1,L} = \\ &= X_{u,R,v-1,L}^{s-1,L,t,R} = X_{u-1,L,v,R}^{s,R,t-1,L} = X_{u-1,L,v-1,L}^{s-1,L,t-1,L}. \end{aligned} \quad (4.8)$$

In case only the upper position indices are the same ($s = t \neq u \neq v$) one arrives at

$$\begin{aligned} X_{u,R,v,R}^{s,R,s,R} &= X_{u-1,L,v,R}^{s,R,s,R} = X_{u,R,v-1,L}^{s-1,L,s-1,L} = X_{u,R,v-1,L}^{s,R,s,R} = X_{u-1,L,v,R}^{s-1,L,s-1,L} = \\ &= X_{u,R,v,R}^{s-1,L,s-1,L} = X_{u-1,L,v-1,L}^{s,R,s,R} = X_{u-1,L,v-1,L}^{s-1,L,s-1,L}, \\ X_{u,R,v,R}^{s-1,L,s,R} &= X_{u-1,L,v-1,L}^{s,R,s-1,L} = X_{u,R,v,R}^{s,R,s-1,L} = X_{u-1,L,v-1,L}^{s-1,L,s,R} = X_{u-1,L,v,R}^{s-1,L,s,R} = \\ &= X_{u,R,v-1,L}^{s,R,s-1,L} = X_{u,R,v-1,L}^{s-1,L,s,R} = X_{u-1,L,v,R}^{s,R,s-1,L}. \end{aligned} \quad (4.9)$$

The row of equations (4.8) splits similarly into 2 rows also for the cases when any other two indices are the same and the rest is different.

For the case when there are two pairs of identical indices, for example $s = t \neq u = v$ the shift conditions become

$$\begin{aligned} X_{u,R,u,R}^{s,R,s,R} &= X_{u,R,u,R}^{s-1,L,s-1,L} = X_{u-1,L,u-1,L}^{s,R,s,R} = X_{u-1,L,u-1,L}^{s-1,L,s-1,L}, \\ X_{u,R,u,R}^{s-1,L,s,R} &= X_{u-1,L,u-1,L}^{s,R,s-1,L} = X_{u,R,u,R}^{s,R,s-1,L} = X_{u-1,L,u-1,L}^{s-1,L,s,R}, \\ X_{u-1,L,u,R}^{s,R,s,R} &= X_{u,R,u-1,L}^{s-1,L,s-1,L} = X_{u,R,u-1,L}^{s,R,s,R} = X_{u-1,L,u,R}^{s-1,L,s-1,L}, \\ X_{u-1,L,u,R}^{s-1,L,s,R} &= X_{u,R,u-1,L}^{s,R,s-1,L} = X_{u,R,u-1,L}^{s-1,L,s,R} = X_{u-1,L,u,R}^{s,R,s-1,L}. \end{aligned} \quad (4.10)$$

Again, the row of equations (4.8) splits similarly into 4 parts also for the rest of the cases with two pairs of same indices.

In case there are three identical indices, the row of shift equations again splits into 4 rows, for example for $s = t = u \neq v$ in the following way

$$\begin{aligned} X_{s,R,v,R}^{s,R,s,R} &= X_{s-1,L,v,R}^{s-1,L,s-1,L} = X_{s,R,v-1,L}^{s,R,s,R} = X_{s-1,L,v-1,L}^{s-1,L,s-1,L}, \\ X_{s,R,v,R}^{s-1,L,s,R} &= X_{s-1,L,v-1,L}^{s,R,s-1,L} = X_{s-1,L,v,R}^{s,R,s-1,L} = X_{s,R,v-1,L}^{s-1,L,s,R}, \\ X_{s-1,L,v,R}^{s,R,s,R} &= X_{s,R,v-1,L}^{s-1,L,s-1,L} = X_{s-1,L,v-1,L}^{s,R,s,R} = X_{s,R,v-1,L}^{s-1,L,s-1,L}, \\ X_{s,R,v,R}^{s,R,s-1,L} &= X_{s,R,v-1,L}^{s,R,s-1,L} = X_{s-1,L,v-1,L}^{s-1,L,s,R} = X_{s-1,L,v,R}^{s-1,L,s,R}. \end{aligned} \quad (4.11)$$

Finally for the diagonal terms, i.e. when $s = t = u = v$, one gets

$$\begin{aligned}
X_{s,R,s,R}^{s,R,s,R} &= X_{s-1,L,s-1,L}^{s-1,L,s-1,L}, & X_{s,R,s,R}^{s-1,L,s,R} &= X_{s-1,L,s-1,L}^{s,R,s-1,L}, \\
X_{s-1,L,s,R}^{s,R,s,R} &= X_{s,R,s-1,L}^{s-1,L,s-1,L}, & X_{s-1,L,s,R}^{s-1,L,s,R} &= X_{s,R,s-1,L}^{s,R,s-1,L}, \\
X_{s,R,s,R}^{s-1,L,s-1,L} &= X_{u-1,L,u-1,L}^{s,R,s,R}, & X_{s,R,s,R}^{s,R,s-1,L} &X_{s-1,L,s-1,L}^{s-1,L,s,R}, \\
X_{s,R,s-1,L}^{s,R,s,R} &= X_{s-1,L,s,R}^{s-1,L,s-1,L}, & X_{s,R,s-1,L}^{s-1,L,s,R} &= X_{s-1,L,s,R}^{s,R,s-1,L},
\end{aligned} \tag{4.12}$$

so this time the row of equations splits completely into 8 parts.

4.1.1 Boundary conditions

As a small reminder, the difference between the finite line and the circle is again in the boundary conditions, which are applied to the shift conditions. For the finite line of length N , **reflecting boundary conditions** are applied, where edges $(-1, 0)$ and $(N - 1, N)$ remain permanently broken. In this case all of the above mentioned shift conditions are valid for all $s, t, u, v \in \{1, 2, \dots, N - 1\}$.

For the case of the circle the **periodic boundary conditions** are applied through identification $0 \equiv N$. With this, all of the shift conditions hold for all $s, t, u, v \in \{0, 1, 2, \dots, N - 1\}$. This means, that an attractor on the circle also has to satisfy the shift conditions for the line plus some additional ones for the cases when any of the position indices are 0. Consequently, any attractor for the circle must also be an attractor for the finite line.

4.2 Coin condition

For two particles the coin conditions are the following

$$(RC \otimes RC)X(RC \otimes RC)^\dagger = \lambda X, \quad \lambda \in \mathbb{C}. \tag{4.13}$$

As a result of the block structure of the attractors, this condition can again be solved for individual attractor blocks $X_{(u,v)}^{(s,t)}$ as

$$(\mathcal{R}H \otimes \mathcal{R}H)X_{(u,v)}^{(s,t)}(\mathcal{R}H \otimes \mathcal{R}H)^\dagger = \lambda X_{(u,v)}^{(s,t)}, \quad \lambda \in \mathbb{C}. \tag{4.14}$$

An important role in this case plays the tensor product structure of the coin condition. As has been mentioned previously, the operator

$$\mathcal{R}H = \frac{1}{\sqrt{2}} \begin{pmatrix} 1 & -1 \\ 1 & 1 \end{pmatrix}, \tag{4.15}$$

has two eigenvalues and their respective orthonormal eigenvectors are the following

$$\begin{aligned}
\lambda_+ = \frac{1}{\sqrt{2}}(1 + i) : & \quad |+\rangle = \frac{1}{\sqrt{2}} \begin{pmatrix} i \\ 1 \end{pmatrix} = \frac{1}{\sqrt{2}}(i|L\rangle + |R\rangle), \\
\lambda_- = \frac{1}{\sqrt{2}}(1 - i) : & \quad |-\rangle = \frac{1}{\sqrt{2}} \begin{pmatrix} -i \\ 1 \end{pmatrix} = \frac{1}{\sqrt{2}}(-i|L\rangle + |R\rangle).
\end{aligned} \tag{4.16}$$

That means that the operator $(\mathcal{R}H \otimes \mathcal{R}H)$ then has eigenvalues $\{1, i, -i\}$ and their respective eigenvectors are

$$\begin{aligned}
\lambda_{++} = \lambda_+ \lambda_+ = i : & \quad \{|+\rangle \otimes |+\rangle \equiv |++\rangle\}, \\
\lambda_{+-} = \lambda_+ \lambda_- = 1 : & \quad \{|+\rangle \otimes |-\rangle \equiv |+-\rangle, |-\rangle \otimes |+\rangle \equiv |-+\rangle\}, \\
\lambda_{--} = \lambda_- \lambda_- = -i : & \quad \{|-\rangle \otimes |-\rangle \equiv |--\rangle\}.
\end{aligned} \tag{4.17}$$

From that the possible eigenvalues λ of the operator (4.13) can be obtained as $\{1, i, -i, -1\}$ together with the corresponding eigenbasis of the general attractor blocks as

$$\begin{aligned}
\lambda_1 = 1 : & \quad \{|+-\chi+-\rangle, |+-\chi-\rangle, |+-\chi+\rangle, |+-\chi--\rangle, |++\chi++\rangle, |--\chi--\rangle\}, \\
\lambda_2 = i : & \quad \{|++\chi+-\rangle, |++\chi-\rangle, |+-\chi--\rangle, |+-\chi--\rangle\}, \\
\lambda_3 = -i : & \quad \{|--\chi+-\rangle, |--\chi-\rangle, |+-\chi++\rangle, |+-\chi++\rangle\}, \\
\lambda_4 = -1 : & \quad \{|++\chi--\rangle, |--\chi++\rangle\}.
\end{aligned} \tag{4.18}$$

However a more simple basis can be found, in which the general attractor blocks of the aforementioned eigenvalues can be written as

$$\lambda_1 = 1 : X_{(u,v)}^{(s,t)} = \begin{pmatrix} a & -b & -c & d \\ -e & f & a-d-f & -b-c-e \\ b+c+e & a-d-f & f & e \\ d & c & b & a \end{pmatrix}, \tag{4.19}$$

$$\lambda_2 = i : X_{(u,v)}^{(s,t)} = \begin{pmatrix} -d & a & b & -ia-ib-d \\ c & -ia-ic-d & -ib-ic-d & -a-b-c+2id \\ -a-b-c+2id & ib+ic+d & ia+ic+d & c \\ ia+ib+d & b & a & d \end{pmatrix}, \tag{4.20}$$

$$\lambda_3 = -i : X_{(u,v)}^{(s,t)} = \begin{pmatrix} -d & a & b & ia+ib-d \\ c & +ia+ic-d & +ib+ic-d & -a-b-c-2id \\ -a-b-c-2id & -ib-ic+d & -ia-ic+d & c \\ -ia-ib+d & b & a & d \end{pmatrix}, \tag{4.21}$$

$$\lambda_4 = -1 : X_{(u,v)}^{(s,t)} = \begin{pmatrix} a & -b & -b & -a \\ -b & -a & -a & b \\ -b & -a & -a & b \\ -a & b & b & a \end{pmatrix}. \tag{4.22}$$

This basis will now be used for the rest of this work.

4.3 Finding p-attractors

Starting again with the p-attractors, lets take a general common eigenvector of the form

$$|\psi\rangle = \sum_{s,t=0}^{N-1} \sum_{c,d \in \{L,R\}} \psi_{s,c,t,d} |s, c, t, d\rangle. \tag{4.23}$$

Then the amplitudes $\psi_{s,c,t,d}$ have to satisfy the following shift conditions

$$s \neq t : \quad \psi_{s,R,t,R} = \psi_{s-1,L,t,R} = \psi_{s,R,t-1,L} = \psi_{s-1,L,t-1,L}, \tag{4.24}$$

$$\begin{aligned}
s = t : \quad \psi_{s,R,s,R} &= \psi_{s-1,L,s-1,L}, \\
\psi_{s-1,L,s,R} &= \psi_{s,R,s-1,L}.
\end{aligned} \tag{4.25}$$

It is obvious, that if one takes two one-particle common eigenstates, then their tensor product is again a two-particle common eigenstate. It can be easily shown, that the resulting common eigenstates then satisfy stricter shift conditions, namely condition (4.24) holds even for the case $s = t$. Clearly any linear combination of these separable common eigenstates will satisfy these conditions as well. The situation is the same when constructing two-particle p-attractors from one-particle p-attractors. In conclusion, a certain subspace of the two-particle attractors, but not necessarily the whole attractor space, can always be constructed purely from one-particle dynamic. It will be shown, that the same holds for non-p-attractors. The remaining problem is then whether there are any additional attractors, which do not satisfy these stricter 'separable' shift conditions. That means attractors which can not be constructed from one-particle attractors.

In case of one particle on a finite line with $\mathcal{R} = \sigma_x$ and the Hadamard coin as a local coin operator there are, as has been shown earlier, altogether two common eigenstates, one for each eigenvalue of $\mathcal{R}H$

$$\begin{aligned}\lambda_+ = \frac{1}{\sqrt{2}}(1 + i) : \quad |\phi_+\rangle &= \frac{1}{\sqrt{N}} \sum_{s=0}^{N-1} (-i)^s |s, +\rangle, \\ \lambda_- = \frac{1}{\sqrt{2}}(1 - i) : \quad |\phi_-\rangle &= \frac{1}{\sqrt{N}} \sum_{s=0}^{N-1} (i)^s |s, -\rangle.\end{aligned}\quad (4.26)$$

From these one-walker common eigenstates four two-particle common eigenstates can be constructed

$$\begin{aligned}\lambda_{++} = i : \quad |\Phi_{++}\rangle &= |\phi_+\rangle \otimes |\phi_+\rangle = \frac{1}{N} \sum_{s,t=0}^{N-1} (-i)^{s+t} |s, +, t, +\rangle, \\ \lambda_{--} = -i : \quad |\Phi_{--}\rangle &= |\phi_-\rangle \otimes |\phi_-\rangle = \frac{1}{N} \sum_{s,t=0}^{N-1} (i)^{s+t} |s, -, t, -\rangle, \\ \lambda_{+-} = 1 : \quad |\Phi_{+-}\rangle &= |\phi_+\rangle \otimes |\phi_-\rangle = \frac{1}{N} \sum_{s,t=0}^{N-1} (-1)^s (i)^{s+t} |s, +, t, -\rangle, \\ |\Phi_{-+}\rangle &= |\phi_-\rangle \otimes |\phi_+\rangle = \frac{1}{N} \sum_{s,t=0}^{N-1} (-1)^t (i)^{s+t} |s, -, t, +\rangle.\end{aligned}\quad (4.27)$$

However, for the eigenvalue $\lambda_{+-} = 1$ there is one more linearly independent (but not orthogonal) non-separable common eigenstate

$$|\Phi_w\rangle = \frac{1}{\sqrt{2N}} \sum_{s=0}^{N-1} (|s, +, s, -\rangle + |s, -, s, +\rangle). \quad (4.28)$$

The rest of this section will be concerned with proving, that these are indeed all common eigenstates. For $\lambda_{++} = i$ one gets a general common eigenvector of the form

$$|\psi\rangle = \sum_{s,t=0}^{N-1} a_{s,t} |s, +, t, +\rangle, \quad (4.29)$$

where amplitudes $a_{s,t}$ have to satisfy conditions (4.24) and (4.25). That means that

$$s \neq t : \quad a_{s,t} = ia_{s-1,t} = ia_{s,t-1} = -a_{s-1,t-1}, \quad (4.30)$$

$$\begin{aligned}s = t : \quad a_{s,s} &= -a_{s-1,s-1}, \\ a_{s-1,s} &= a_{s,s-1}.\end{aligned}\quad (4.31)$$

From this it is obvious, that if one sets a_{00} , the rest of the amplitudes are set as well. This means that $\lambda_{++} = i$ truly only has one common eigenstate $|\Phi_{++}\rangle$ mentioned earlier.

Similarly for $\lambda_{--} = -i$ the conditions become

$$s \neq t : a_{s,t} = -ia_{s-1,t} = -ia_{s,t-1} = -a_{s-1,t-1,L}, \quad (4.32)$$

$$\begin{aligned} s = t : a_{s,s} &= -a_{s-1,s-1}, \\ a_{s-1,s} &= a_{s,s-1}, \end{aligned} \quad (4.33)$$

for general common eigenvector

$$|\psi\rangle = \sum_{s,t=0}^{N-1} a_{s,t} |s, -, t, -\rangle. \quad (4.34)$$

So it is again clear, that this eigenspace is also one dimensional with only one common eigenstate $|\Phi_{--}\rangle$. For both i and $-i$ the equations for amplitudes can be easily solved and the results will truly be $|\Phi_{++}\rangle$ and $|\Phi_{--}\rangle$.

For eigenvalue $\lambda_{+-} = 1$ the situation gets a bit more complicated. There is now two dimensional subspace of possible coin states ($\{|+-\rangle, | -+\rangle\}$), which means, that general common eigenstate now has the form

$$|\psi\rangle = \sum_{s,t=0}^{N-1} a_{s,t} |s, +, t, -\rangle + b_{s,t} |s, -, t, +\rangle. \quad (4.35)$$

The shift conditions give us the following sets of equations for amplitudes $a_{s,t}, b_{s,t}$

$$\begin{aligned} s = t : \quad & \psi_{s,L,s,L} = \psi_{s+1,R,s+1,R} \rightarrow a_{s,s} + b_{s,s} = a_{s+1,s+1} + b_{s+1,s+1}, \\ & \psi_{s,L,s+1,R} = \psi_{s+1,R,s,L} \rightarrow -a_{s+1,s} + b_{s+1,s} = a_{s,s+1} - b_{s,s+1}, \\ & \psi_{s,L,s,R} = \psi_{s+1,R,s,R} \rightarrow a_{s+1,s} + b_{s+1,s} = -i(a_{s,s} - b_{s,s}), \\ & \psi_{s,R,s,L} = \psi_{s,R,s+1,R} \rightarrow a_{s,s+1} + b_{s,s+1} = i(a_{s,s} - b_{s,s}), \\ & \psi_{s+1,L,s+1,R} = \psi_{s+1,L,s,L} \rightarrow a_{s+1,s} + b_{s+1,s} = -i(a_{s+1,s+1} - b_{s+1,s+1}), \\ & \psi_{s+1,R,s+1,L} = \psi_{s,L,s+1,L} \rightarrow a_{s,s+1} + b_{s,s+1} = i(a_{s+1,s+1} - b_{s+1,s+1}), \\ s \neq t : \quad & \psi_{s,L,t,L} = \psi_{s+1,R,t+1,R} \rightarrow a_{s,t} + b_{s,t} = a_{s+1,t+1} + b_{s+1,t+1}, \\ & \psi_{s,L,t+1,R} = \psi_{s+1,R,t,L} \rightarrow -a_{s+1,t} + b_{s+1,t} = a_{s,t+1} - b_{s,t+1}, \\ & \psi_{s,L,t,R} = \psi_{s+1,R,t,R} \rightarrow a_{s+1,t} + b_{s+1,t} = -i(a_{s,t} - b_{s,t}), \\ & \psi_{s,R,t,L} = \psi_{s,R,t+1,R} \rightarrow a_{s,t+1} + b_{s,t+1} = i(a_{s,t} - b_{s,t}), \\ & \psi_{s+1,L,t+1,R} = \psi_{s+1,L,t,L} \rightarrow a_{s+1,t} + b_{s+1,t} = -i(a_{s+1,t+1} - b_{s+1,t+1}), \\ & \psi_{s+1,R,t+1,L} = \psi_{s,L,t+1,L} \rightarrow a_{s,t+1} + b_{s,t+1} = i(a_{s+1,t+1} - b_{s+1,t+1}), \\ & \psi_{s,L,t,L} = \psi_{s,L,t+1,R} \rightarrow a_{s,t} + b_{s,t} = -i(a_{s,t+1} - b_{s,t+1}). \end{aligned} \quad (4.36)$$

One can see that for non-diagonal terms the only difference is one additional independent equation. These sets of equations can be simplified to

$$\begin{aligned} s = t : \quad & -ia_{s,s} + ib_{s,s} - a_{s,s+1} = b_{s,s+1} = -b_{s+1,s}, \\ & -a_{s+1,s} = a_{s,s+1}, \\ & a_{s+1,s+1} = a_{s,s}, \\ & b_{s+1,s+1} = b_{s,s}, \\ s \neq t : \quad & a_{s,t} = -ib_{s,t+1} = ib_{s+1,t} = a_{s+1,t+1}, \\ & b_{s,t} = -ia_{s,t+1} = ia_{s+1,t} = b_{s+1,t+1}. \end{aligned}$$

From this it is clear, that if a_{00}, a_{01}, b_{00} are set, the rest of the amplitudes are set as well. The subspace of common eigenstates corresponding to the eigenvalue $\lambda_{+-} = 1$ is then three dimensional. We can get the vectors $|\Phi_{+-}\rangle, |\Phi_{-+}\rangle, |\Phi_w\rangle$ from following linearly independent settings:

$$\begin{aligned} |\Phi_{+-}\rangle : \quad a_{00} &= \frac{1}{N}; \quad a_{01} = \frac{i}{N}; \quad b_{00} = 0, \\ |\Phi_{-+}\rangle : \quad a_{00} &= a_{01} = 0; \quad b_{00} = \frac{1}{N}, \\ |\Phi_w\rangle : \quad a_{00} &= b_{00} = \frac{1}{\sqrt{2N}}; \quad a_{01} = 0. \end{aligned}$$

In conclusion, there is the following orthonormal eigenbasis of common eigenstates

$$\begin{aligned} \lambda_{++} &= i : \quad |\Phi_{++}\rangle, \\ \lambda_{--} &= -i : \quad |\Phi_{--}\rangle, \\ \lambda_{+-} &= 1 : \quad |\Phi_{+-}\rangle, \\ \lambda_{+-} &= 1 : \quad |\Phi_{+-}\rangle, |\Phi_{-+}\rangle, |\Phi_w\rangle \equiv \sqrt{\frac{N}{N-1}} \left[|\Phi_w\rangle - \frac{1}{\sqrt{2N}} (|\Phi_{+-}\rangle + |\Phi_{-+}\rangle) \right]. \end{aligned} \quad (4.38)$$

From that follows, that 25 p-attractors in total can be constructed

$$\begin{aligned} \lambda_1 = 1 : \quad & \{ |\Phi_{++}\rangle\langle\Phi_{++}|, |\Phi_{--}\rangle\langle\Phi_{--}|, |\Phi_{+-}\rangle\langle\Phi_{+-}|, |\Phi_{-+}\rangle\langle\Phi_{-+}|, |\Phi_{+-}\rangle\langle\Phi_{-+}|, |\Phi_{-+}\rangle\langle\Phi_{+-}|, \\ & |\Phi_w\rangle\langle\Phi_{+-}|, |\Phi_w\rangle\langle\Phi_{-+}|, |\Phi_{+-}\rangle\langle\Phi_w|, |\Phi_{-+}\rangle\langle\Phi_w|, |\Phi_w\rangle\langle\Phi_w| \}, \\ \lambda_2 = i : \quad & \{ |\Phi_{+-}\rangle\langle\Phi_{--}|, |\Phi_{-+}\rangle\langle\Phi_{--}|, |\Phi_w\rangle\langle\Phi_{--}|, |\Phi_{++}\rangle\langle\Phi_{+-}|, |\Phi_{++}\rangle\langle\Phi_{-+}|, |\Phi_{++}\rangle\langle\Phi_w| \}, \\ \lambda_3 = -i : \quad & \{ |\Phi_{+-}\rangle\langle\Phi_{++}|, |\Phi_{-+}\rangle\langle\Phi_{++}|, |\Phi_w\rangle\langle\Phi_{++}|, |\Phi_{--}\rangle\langle\Phi_{+-}|, |\Phi_{--}\rangle\langle\Phi_{-+}|, |\Phi_{--}\rangle\langle\Phi_w| \}, \\ \lambda_4 = -1 : \quad & \{ |\Phi_{++}\rangle\langle\Phi_{--}|, |\Phi_{--}\rangle\langle\Phi_{++}| \}. \end{aligned} \quad (4.39)$$

4.3.1 Circle

Up until now only the reflecting boundary conditions have been considered, i.e. the finite line of the length N . To determine the p-attractors for the circle one needs to find out, which of the common eigenvectors are periodic.

The periodicity condition for $|\Phi_{++}\rangle, |\Phi_{+-}\rangle, |\Phi_{-+}\rangle, |\Phi_{--}\rangle$ reduces to $(i)^N = i^0 = 1$. This means, that all of these common eigenvectors can be present only for a circle of the length $N = 4k, \forall k \in \mathbb{N}$. The only remaining eigenvector $|\Phi_w\rangle$ has position independent amplitudes, so it will be present for circles of all lengths.

In conclusion, for circles of length $N = 4k, \forall k \in \mathbb{N}$ the situation is identical to the case of a line. For $N \neq 4k$ there is only one common eigenstate $|\Phi_w\rangle$ for the eigenvalue 1.

4.4 Non-p-attractors

For one particle, the only non-p-attractor is the identity $I^{(1)}$. However, for the two-particle quantum walk quite a significant amount of non-p-attractors appears. As will be shown later, in this case it is actually possible to construct all of the remaining non-p-attractors using one-particle attractors.

Tensor product of two one-particle attractors is a two-particle attractor. If at least one of the one-particle attractors is a non-p-attractor, then the resulting two-particle attractor is also a non-p-attractor.

With this knowledge, one can construct the following 9 linearly independent non-p-attractors

$$\begin{aligned}
\lambda_1 = 1 : & \quad \{I^{(1)} \otimes |\phi_+ \rangle \langle \phi_+|, I^{(1)} \otimes |\phi_- \rangle \langle \phi_-|, |\phi_+ \rangle \langle \phi_+| \otimes I^{(1)}, |\phi_- \rangle \langle \phi_-| \otimes I^{(1)}, I = I^{(1)} \otimes I^{(1)}\}, \\
\lambda_2 = i : & \quad \{I^{(1)} \otimes |\phi_- \rangle \langle \phi_+|, |\phi_- \rangle \langle \phi_+| \otimes I^{(1)}\}, \\
\lambda_3 = -i : & \quad \{I^{(1)} \otimes |\phi_+ \rangle \langle \phi_-|, |\phi_+ \rangle \langle \phi_-| \otimes I^{(1)}\}.
\end{aligned} \tag{4.40}$$

Global identity I can be normalized by $1/2N$ and the rest of them by $1/\sqrt{2N}$. It follows from the fact that $\text{Tr}[X \otimes Y] = \text{Tr}_1[X] \text{Tr}_1[Y]$, where Tr_1 is a partial trace over one-particle space.

To get the rest of the non-p-attractors, a new operator needs to be introduced

$$W = \sum_{s,t=0}^{N-1} \sum_{c,d \in \{L,R\}} |s, c, t, d \rangle \langle t, d, s, c|. \tag{4.41}$$

When closely examined, this is clearly an operator which swaps the two particles, from this reason it will be sometimes referred as the SWAP operator from now on. It has the following properties: $W = W^\dagger$ and $WW^\dagger = W^2 = I$. It can then also be easily shown, that for any one-particle operators X, Y it holds that

$$W(X \otimes Y)W = X \otimes Y \implies [W, U \otimes U] = 0. \tag{4.42}$$

From that follows, that if X is an attractor with the respective eigenvalue $\lambda \in \mathbb{C}$, WX is also an attractor belonging to the eigenvalue λ

$$(U \otimes U)WX(U \otimes U)^\dagger = W(U \otimes U)X(U \otimes U)^\dagger = W\lambda X = \lambda(WX). \tag{4.43}$$

With this knowledge, another 9 non-p-attractors can now be constructed by multiplying all of the attractors (4.40) with W . This new set is again linearly independent because

$$\langle WX, WY \rangle_{HS} = \text{Tr}[(WX)^\dagger(WY)] = \text{Tr}[X^\dagger WWY] = \text{Tr}[X^\dagger Y] = \langle X, Y \rangle_{HS}. \tag{4.44}$$

The remaining question is, whenever the new non-p-attractors and the original ones are linearly independent, i.e. if one get any new non-p-attractors by this procedure. Straightforward calculation reveals, that

$$\begin{aligned}
\langle W(I^{(1)} \otimes X), (I^{(1)} \otimes Y) \rangle_{HS} &= \text{Tr}[(W(I^{(1)} \otimes X))^\dagger(I^{(1)} \otimes Y)] = \\
&= \text{Tr}_1[X^\dagger Y] = \langle X, Y \rangle_{HS_1}.
\end{aligned} \tag{4.45}$$

The same also holds for other forms of non-p-attractors

$$\begin{aligned}
\langle W(X \otimes I^{(1)}), (I^{(1)} \otimes Y) \rangle_{HS} &= \langle W(I^{(1)} \otimes X), (Y \otimes I^{(1)}) \rangle_{HS} = \\
&= \langle W(X \otimes I^{(1)}), (Y \otimes I^{(1)}) \rangle_{HS} = \langle X, Y \rangle_{HS_1}.
\end{aligned} \tag{4.46}$$

It is therefore clear, since all of the one-particle p-attractors X, Y are orthonormal, that this indeed yielded new linearly independent non-p-attractors. They are also orthogonal with the original ones except for cases $X = Y$ and for the cases when global identity is involved. After normalizing the first 9 attractors the norm does not change by applying the W operator, so the new 9 attractors will also be normalized. This means there are in total 4 non-p-attractors for $\lambda_2 = i$, 4 for $\lambda_3 = -i$ and 10 for $\lambda_4 = 1$.

4.4.1 Circle

All of the one-particle p-attractors satisfy the periodicity condition only for $N = 4k, \forall k \in \mathbb{N}$. In that case there are all of the non-p-attractors constructed above. In cases $N \neq 4k, \forall k \in \mathbb{N}$ only one non-p-attractor remains and that is the global identity I and consequently also the operator W .

4.4.2 Summary and orthonormal basis

Together with the p-attractors that makes 21 attractors for the eigenvalue 1, 10 for i , 10 for $-i$ and 2 for -1 . So in total there are **43 attractors** for two particles on the finite line of length N and also for the circles of lengths $N \neq 4k, \forall k \in \mathbb{N}$. For the circles of lengths $N \neq 4k, \forall k \in \mathbb{N}$ there are in total only **3 attractors** and that is I, W and $|\Phi_w\rangle\langle\Phi_w|$. Compared to the one-particle case it is interesting to notice two things. First interesting thing is the great number of non-p-attractors for the two-particle case while there is only the identity for the one-particle case. The total number of attractors is still fixed for all lengths N , as it has been the case for one walker as well, however the number is much greater. Second is that a lot of the attractors in the non-interacting two-particle case can be constructed from the one-particle attractors, however interestingly not all of them. The parts of the solution that cannot be obtained from the one-particle results are connected to the entangled common eigenvector $|\Phi_w\rangle$. This eigenvector is then involved in the construction of altogether 9 of the total of 25 p-attractors. In the non-p-attractor the purely two-particle effects are introduced together with the SWAP operator W . The appearance of W can actually be deduced from the fact that states called the Werner states, first introduced in [41], are always the solution of the non-interacting percolation problem. Two-particle Werner states \tilde{W} are defined as such density matrices that satisfy

$$(U \otimes U)\tilde{W}(U \otimes U)^\dagger = \tilde{W}, \quad (4.47)$$

for all unitary operators U on a given Hilbert space of the system. So they are states invariant towards all possible unitary operations. By looking at the conditions on attractors (4.2) every Werner state is clearly an attractor. It can also be shown that two-particle Werner states can be written down as the linear combination of the global identity I and the SWAP operator W . So clearly all Werner states are truly included in the found group of attractors.

As has been shown earlier, the found non-p-attractors do not form an orthonormal set despite being linearly independent. The p-attractors do form an orthonormal set, however they are not orthogonal to the non-p-attractors. They always overlap with at least one of the non-p-attractors. So in order to get the orthonormal basis of the whole attractor space one has to orthogonalize the whole set of 43 attractors for the finite line. That is quite a time-consuming task, so only the overlaps of the p-attractors with the non-p-attractors will be presented. From these it is possible to orthogonalize the whole set using the linearity of trace.

The overlapping of the found attractors will now be briefly shown. As has been said earlier the p-attractors are orthonormal in between each other, so let's look at the overlaps of p-attractors with non-p-attractors. Considering the p-attractors constructed only from the separable common eigestates first,

one gets the following formulas

$$\begin{aligned}
\left\langle (|\Phi_{kk'}\rangle\langle\Phi_{l'l'}|), \frac{1}{\sqrt{2N}} \left(I^{(1)} \otimes |\phi_m\rangle\langle\phi_{m'}| \right) \right\rangle_{HS} &= \frac{1}{\sqrt{2N}} \text{Tr} \left[(|\Phi_{kk'}\rangle\langle\Phi_{l'l'}|)^\dagger \left(I^{(1)} \otimes |\phi_m\rangle\langle\phi_{m'}| \right) \right] = \\
&= \frac{1}{\sqrt{2N}} \text{Tr} \left[(|\phi_l\rangle \otimes |\phi_{l'}\rangle) \langle\langle\phi_k| \otimes \langle\phi_{k'}| \rangle \left(I^{(1)} \otimes |\phi_m\rangle\langle\phi_{m'}| \right) \right] = \\
&= \frac{1}{\sqrt{2N}} \text{Tr} \left[|\phi_k\rangle\langle\phi_l| \otimes (|\phi_{k'}\rangle\langle\phi_{l'}| |\phi_m\rangle\langle\phi_{m'}|) \right] = \\
&= \frac{1}{\sqrt{2N}} \delta_{l'm} \delta_{kl} \delta_{k'l'}, \\
\left\langle (|\Phi_{kk'}\rangle\langle\Phi_{l'l'}|), \frac{1}{\sqrt{2N}} \left(|\phi_m\rangle\langle\phi_{m'}| \otimes I^{(1)} \right) \right\rangle_{HS} &= \dots = \frac{1}{\sqrt{2N}} \delta_{lm'} \delta_{k'l'} \delta_{km}, \\
\left\langle (|\Phi_{kk'}\rangle\langle\Phi_{l'l'}|), \frac{1}{\sqrt{2N}} \left(|\phi_m\rangle\langle\phi_{m'}| \otimes I^{(1)} \right) \right\rangle_{HS} &= \dots = \frac{1}{\sqrt{2N}} \delta_{lm'} \delta_{k'l'} \delta_{km}, \\
\left\langle (|\Phi_{kk'}\rangle\langle\Phi_{l'l'}|), \frac{1}{2N} I \right\rangle_{HS} &= \dots = \frac{1}{2N} \delta_{kl} \delta_{k'l'}, \tag{4.48}
\end{aligned}$$

where $k, k', l, l', m, m' \in \{+, -\}$. For the other 9 non-p-attractors with the SWAP operator (4.41) the formulas are very similar, the only change is $l \leftrightarrow l'$. So clearly there are some non-zero overlaps of the separable p-attractors with different non-p-attractors.

For the p-attractors containing $|\Phi'_w\rangle$ the situation becomes a bit more complicated. It is easier to first look at the overlaps of non-p-attractors with different p-attractors constructed from $|\Phi_w\rangle$, which can be shown to be

$$\begin{aligned}
\left\langle |\Phi_w\rangle\langle\Phi_w|, \left(\frac{I^{(1)}}{\sqrt{2N}} \otimes |\phi_k\rangle\langle\phi_m| \right) \right\rangle_{HS} &= \left\langle |\Phi_w\rangle\langle\Phi_w|, \left(|\phi_k\rangle\langle\phi_m| \otimes \frac{I^{(1)}}{\sqrt{2N}} \right) \right\rangle_{HS} = \dots = \frac{1}{(2N)^{3/2}}, \\
\left\langle |\Phi_{kl}\rangle\langle\Phi_w|, \left(\frac{I^{(1)}}{\sqrt{2N}} \otimes |\phi_m\rangle\langle\phi_n| \right) \right\rangle_{HS} &= \left\langle |\Phi_{lk}\rangle\langle\Phi_w|, \left(|\phi_m\rangle\langle\phi_n| \otimes \frac{I^{(1)}}{\sqrt{2N}} \right) \right\rangle_{HS} = \dots = \frac{1}{2N} \delta_{nl}, \\
\left\langle |\Phi_w\rangle\langle\Phi_{kl}|, \left(\frac{I^{(1)}}{\sqrt{2N}} \otimes |\phi_m\rangle\langle\phi_n| \right) \right\rangle_{HS} &= \left\langle |\Phi_w\rangle\langle\Phi_{lk}|, \left(|\phi_m\rangle\langle\phi_n| \otimes \frac{I^{(1)}}{\sqrt{2N}} \right) \right\rangle_{HS} = \dots = \frac{1}{2N} (1 - \delta_{nl}), \tag{4.49}
\end{aligned}$$

where $k, l, m, n \in \{+, -\}$. For the non-p-attractors with SWAP operator one only applies the SWAP to the p-attractors from the left in the trace formula and then uses the formulas above. This is easier since for the separable p-attractors it only switches the one-particle p-attractors and $|\Phi_w\rangle$ is invariant towards the SWAP. The overlaps with p-attractors containing $|\Phi_w\rangle$ can then be constructed from these due to linearity.

Then there are of course overlaps in between the non-p-attractors themselves. Without the SWAP operator the situation for the first 9 non-p-attractors looks simply as

$$\begin{aligned}
\left\langle X \otimes \frac{I^{(1)}}{\sqrt{2N}}, Y \otimes \frac{I^{(1)}}{\sqrt{2N}} \right\rangle_{HS} &= \left\langle \frac{I^{(1)}}{\sqrt{2N}} \otimes X, \frac{I^{(1)}}{\sqrt{2N}} \otimes Y \right\rangle_{HS} = \text{Tr}_1 [X^\dagger Y] \text{Tr}_1 \left[\frac{I^{(1)}}{2N} \right] = \text{Tr}_1 [X^\dagger Y], \\
\left\langle X \otimes \frac{I^{(1)}}{\sqrt{2N}}, \frac{I^{(1)}}{\sqrt{2N}} \otimes Y \right\rangle_{HS} &= \frac{1}{2N} \text{Tr}_1 [X^\dagger] \text{Tr}_1 [Y], \tag{4.50}
\end{aligned}$$

where X and Y are the one-particle attractors. So clearly there will be certain overlaps in between the first 9 non-p-attractors. Especially for the combinations of one-particle identity and other one-particle non-p-attractors corresponding to the eigenvalue 1, because these have in general non-zero trace. If one

then looks only at the group of the second 9 non-p-attractors which were created via the SWAP operator it turns out that

$$\langle WX, WY \rangle_{HS} = \text{Tr}[(WX)^\dagger(WY)] = \text{Tr}[X^\dagger Y] = \langle X, Y \rangle_{HS}, \quad (4.51)$$

where X and Y now represent arbitrary two-particle attractors. So clearly they will have the same overlaps as the original ones. The question is now the combination of the non-p-attractors from these two groups. Starting with a general formula for one-particle attractors A, B, C, D

$$\begin{aligned} \langle A \otimes B, W(C \otimes D) \rangle_{HS} &= \text{Tr}[(A^\dagger \otimes B^\dagger)W(C \otimes D)] = \sum \bar{A}_{cd}^{ab} \bar{B}_{\tilde{c}\tilde{d}}^{\tilde{a}\tilde{b}} C_{c'd'}^{a'b'} D_{c'd''}^{a''b''} \langle s, t, u, v | c, d, \tilde{c}, \tilde{d} \rangle \\ &\quad \langle a, b, \tilde{a}, \tilde{b} | e, f, e', f' \rangle \langle e', f', e, f | a', b', a'', b'' \rangle \langle c', d', c'', d'' | s, t, u, v \rangle = \\ &= \sum \bar{A}_{cd}^{ab} \bar{B}_{c'd''}^{a'b'} C_{cd}^{ab} D_{c'd''}^{ab}, \end{aligned} \quad (4.52)$$

where the sums are over all present indices in either the position, or the coin space. The indices on the matrix elements of the one-particle attractors follow the same logic as described earlier. So both the upper and the lower ones have the position index first and the coin index second. If one now looks at our special cases where always two of the one-particle attractors are the one-particle identity, the following formulas can be derived

$$\begin{aligned} \langle I \otimes B, W(I \otimes D) \rangle_{HS} &= \text{Tr}_1 [B^\dagger D], \\ \langle A \otimes I, W(C \otimes I) \rangle_{HS} &= \text{Tr}_1 [A^\dagger C], \\ \langle I \otimes B, W(C \otimes I) \rangle_{HS} &= \text{Tr}_1 [B^\dagger C], \\ \langle A \otimes I, W(I \otimes D) \rangle_{HS} &= \text{Tr}_1 [A^\dagger D]. \end{aligned} \quad (4.53)$$

So considering the specific one-particle attractors, there will again be non-zero overlaps for global identity and other attractors corresponding to the eigenvalue 1. This all makes sense when one realizes that the basis for the one-particle attractors was not orthogonal in the first place either exactly for the case of eigenvalue 1.

It is now clear that looking for the orthonormal basis of attractors in the case where the 43 attractors are present would be quite tedious. The construction of the asymptotic states and their analysis would not be better. For this reason the full orthogonalization will later be done only for the case of circles of lengths $N \neq 4k, \forall k \in \mathbb{N}$, where the number of attractors reduces to 3.

4.5 Proof of completeness

This section will show, that there are no more additional non-p-attractors besides the ones that have been constructed so far. The plan is to always start from the block $X_{(0,0)}^{(0,0)}$, which is always fully determined. The next step is then to use the shift conditions to get all of its 15 neighboring blocks ($X_{(0,0)}^{(1,0)}, X_{(0,0)}^{(0,1)}, X_{(0,0)}^{(0,0)}, X_{(0,0)}^{(0,0)}, X_{(0,0)}^{(1,1)}, X_{(0,0)}^{(0,0)}, X_{(0,0)}^{(1,0)}, X_{(0,0)}^{(0,1)}, X_{(0,0)}^{(1,0)}, X_{(0,0)}^{(0,1)}, X_{(0,0)}^{(1,1)}, X_{(0,0)}^{(1,0)}, X_{(0,0)}^{(0,1)}, X_{(0,0)}^{(1,1)}$) while setting as little additional parameters of these neighboring blocks as possible. Some lower bounds on the dimensionality of attractor eigenspaces have been obtained from the previous construction (21 for the eigenvalue 1, 10 for i , 10 for $-i$ and 2 for -1). The goal is now to show that the dimensions can not be higher than that.

The block $X_{(0,0)}^{(0,0)}$ is a diagonal block. As has been shown earlier, this is the block for which the most restricting shift conditions hold. All of the equalities which hold for the diagonal block $X_{(s,s)}^{(s,s)}$ also hold for all of the other types of blocks. For the other blocks one just gets some additional equalities depending

on the type of combination of vertex indices. This means that after determining the first 16 blocks, the rest of the attractor is determined as well. That is the reason why the focus now will only be on $X_{(0,0)}^{(0,0)}$ and its 15 nearest neighbors.

According to the shift conditions

$$\begin{aligned}
X_{0,L,0,L}^{0,L,0,L} &= X_{1,R,1,R}^{1,R,1,R}, \\
X_{0,L,0,L}^{0,R,0,L} &= X_{1,R,1,R}^{0,R,1,R}, & X_{0,L,0,L}^{0,L,0,R} &= X_{1,R,1,R}^{1,R,0,R}, \\
X_{0,R,0,L}^{0,L,0,L} &= X_{0,R,1,R}^{1,R,1,R}, & X_{0,L,0,L}^{0,L,0,L} &= X_{1,R,0,R}^{1,R,1,R}, \\
X_{0,L,0,R}^{0,R,0,R} &= X_{1,R,1,R}^{0,R,0,R}, & X_{0,L,0,L}^{0,L,0,L} &= X_{0,R,0,R}^{1,R,1,R}, \\
X_{0,R,0,L}^{0,R,0,L} &= X_{0,R,1,R}^{0,R,1,R}, & X_{0,L,0,R}^{0,L,0,R} &= X_{1,R,0,R}^{1,R,0,R}, \\
X_{0,L,0,R}^{0,R,0,L} &= X_{1,R,0,R}^{0,R,1,R}, & X_{0,R,0,L}^{0,L,0,R} &= X_{0,R,1,R}^{1,R,0,R}, \\
X_{0,R,0,R}^{0,R,0,R} &= X_{0,R,0,R}^{0,R,0,R}, & X_{0,R,0,L}^{0,R,0,R} &= X_{1,R,0,R}^{0,R,0,R}, \\
X_{0,R,0,L}^{0,R,0,L} &= X_{0,R,1,R}^{0,R,1,R}, & X_{0,L,0,R}^{0,L,0,R} &= X_{1,R,0,R}^{1,R,0,R}.
\end{aligned} \tag{4.54}$$

As can be seen, this always gives us the element X_{RR}^{RR} of one of the neighboring blocks.

Case $\lambda_4 = -1$

The general attractor block (4.22) has two parameters. From conditions (4.54) all of the a parameters (indices note which attractor block do the parameters a and b belong to) can be obtained

$$\begin{aligned}
a_{00}^{00} &= a_{11}^{11} = -a_{01}^{01} = -a_{10}^{10} = -a_{00}^{11} = -a_{11}^{00} = -a_{01}^{10} = -a_{10}^{01}, \\
b_{00}^{00} &= a_{11}^{01} = -a_{11}^{10} = -a_{10}^{11} = -a_{01}^{11} = a_{01}^{00} = -a_{10}^{00} = a_{00}^{01} = a_{00}^{10}.
\end{aligned} \tag{4.55}$$

This means that not only all of the X_{RR}^{RR} elements are known, but also elements $X_{LL}^{LL}, X_{LL}^{RR}, X_{LL}^{RL}, X_{LL}^{LR}, X_{RR}^{RL}, X_{RR}^{LR}, X_{RR}^{LR}, X_{RR}^{RL}$. This knowledge can now be used to get some of the b parameters. Taking what is known about $X_{(00)}^{(10)}$ and using only the shift condition concerning our first 16 blocks gives

$$a_{00}^{10} = b_{11}^{11} = -b_{11}^{00} = -b_{11}^{00} = -b_{10}^{10} = -b_{01}^{01} = -b_{10}^{01} = -b_{01}^{10} (= b_{00}^{00}). \tag{4.56}$$

Getting the rest of the b parameters is a bit more complicated, once one of them is determined, say for example b_{10}^{00} , the rest can also be easily obtained. To see this, one only needs to realize, that if parameter b is known, all of the elements $X_{RR}^{RR}, X_{RR}^{LR}, X_{RR}^{RL}, X_{RR}^{LL}, X_{RR}^{LL}, X_{RR}^{RL}, X_{RR}^{LR}, X_{RR}^{LL}$ are known as well. Using shift conditions on these elements then results in

$$b_{10}^{00} = -b_{00}^{01} = -b_{00}^{10} = -b_{01}^{00} = b_{10}^{11} = b_{11}^{01} = b_{01}^{11} = b_{11}^{10}. \tag{4.57}$$

However, to get b_{10}^{00} , it is necessary to reach for shift conditions beyond the first 16 blocks. Starting with a_{10}^{10} , which is already known, and using some of these shift conditions results in the following series of equations

$$a_{10}^{10} = -b_{20}^{10} = a_{20}^{00} = b_{10}^{00}. \tag{4.58}$$

This has proved that a_{00}^{00} and b_{00}^{00} determines all of the other parameters. Hence, this subspace of attractors is truly only two-dimensional.

Case $\lambda_2 = i$

In this case the general attractor block is given by 4 parameters as the block (4.20). This shows which elements give information about which parameters

$$\begin{array}{ll}
\begin{array}{l}
RR \ LL \\
RR'LL \dots \pm d, \\
LL \ RR \\
RL'LR \dots b, \\
LR \ RL \\
RL'LR \dots \mp (ib + ic + d), \\
LL \ RR \\
RR'LL \dots \mp (ia + ib + d),
\end{array}
&
\begin{array}{l}
RR \ LL \\
RL'LR \dots a, \\
LR \ RL \\
LL'RR \dots c, \\
LR \ RL \\
LR'RL \dots \pm (ia + ic + d), \\
LR \ RL \\
RR'LL \dots -a - b - c + 2id.
\end{array}
\end{array} \tag{4.59}$$

Clearly from $X_{(00)}^{(00)}$ the d parameter of all neighboring blocks can be obtained, but even that knowledge will not help any further. It is necessary to determine some additional parameters. Lets suppose that for example the rest of $X_{(00)}^{(10)}$, that means its a, b and c parameters, are also determined. Applying shift conditions concerning only the first 16 blocks then gives

$$\begin{array}{lll}
X_{0,L,0,L}^{1,R,0,L} = X_{1,R,1,R}^{0,L,1,R}, & X_{0,L,0,L}^{1,R,0,R} = X_{1,R,1,R}^{0,L,0,R}, & X_{0,R,0,L}^{1,R,0,R} = X_{0,R,1,R}^{0,L,0,R}, \\
X_{0,R,0,R}^{1,R,0,L} = X_{1,R,0,R}^{0,L,0,R}, & X_{0,R,0,L}^{1,R,0,L} = X_{1,R,1,R}^{0,L,0,R}, & \dots
\end{array} \tag{4.60}$$

Writing out the rest of the conditions, one can see, that the element $\frac{LR}{RR}$ of the other blocks is always determined as well. This means the value of $(-a - b - c + 2id)$ is known.

Again, some additional blocks now have to be determined, lets take for example the rest of $X_{(00)}^{(11)}$, this means setting for example the parameters a and b . Writing down once again the attached shift conditions as in equations (4.60), one will see, that in this case the elements $\frac{LL}{RR}$ of the remaining blocks are now fixed as well. That means the value of $(ia + ib + d)$ is now known. Together with the previous information about the block parameters this results in the knowledge of the values of d, c and $(a + b)$.

Finally, by setting the parameter a of $X_{(01)}^{(10)}$ the whole block has now been obtained and it is possible to once again use the shift conditions. This time they give the elements $\frac{LR}{RL}$ of the remaining blocks. This means the value of $(ib + ic + d)$ is known which now determines all of the parameters of the remaining blocks.

Overall during this process $4 + 3 + 2 + 1 = 10$ parameters of the first 16 blocks in total needed to be fixed. Meaning the dimension of this eigenspace is maximally 10. Since 10 linearly independent attractors have already been constructed, it is clear that the dimension of this subspace is truly equal to 10.

Case $\lambda_3 = -i$

Taking a close look at the general attractor block (4.21) and comparing it to the block (4.20), which is the general attractor block of the previous case $\lambda_2 = i$, one can see they are almost the same. The only changes are basically the complex conjugations

$$\begin{array}{ll}
(ia + ib + d) & \rightarrow (-a - ib + d), \\
(ia + ic + d) & \rightarrow (-ia - ic + d), \\
(-a - b - c + 2id) & \rightarrow (-a - b - c - 2id).
\end{array}$$

This means that the procedure showing there are truly only 10 attractors in this eigenspace will be completely the same as in the previous case.

Case $\lambda_1 = 1$

At last there is the case of the eigenvalue 1, for which there are the most parameters of the general attractor block (4.19). Specifically, there are 6 for each block: a, b, c, d, e and f . The strategy will be similar as previously and will begin with writing down which parameters can be obtained from which block elements

$$\begin{array}{ll}
 \begin{array}{l}
 \begin{array}{l}
 RR \ LL \\
 RR'LL \dots a, \\
 LL \ RR \\
 RL'LR \dots \pm c, \\
 LR \ RL \\
 LL'RR \dots \pm e, \\
 LR \ RL \\
 RR'LL \dots \mp (b + c + e),
 \end{array}
 &
 \begin{array}{l}
 \begin{array}{l}
 RR \ LL \\
 RL'LR \dots \pm b, \\
 RR \ LL \\
 LL'RR \dots d, \\
 LR \ RL \\
 LR'RL \dots f, \\
 LR \ RL \\
 RL'LR \dots a - d - f.
 \end{array}
 \end{array}
 \end{array}
 \tag{4.61}$$

Next, lets again assume that $X_{(00)}^{(00)}$ is fully set, i.e. all of its 6 parameters are known. From shift conditions (4.54) elements $\begin{smallmatrix} RR \\ RR' \end{smallmatrix}$ of all the neighboring blocks are determined and with that also all of the a parameters. One can not get any further from this, so determining the rest of $X_{(00)}^{(10)}$ elements (so its b, c, d, e and f parameters) is the next step. As previously the $\begin{smallmatrix} LR \\ RR' \end{smallmatrix}$ elements of other blocks from $X_{(00)}^{(10)}$ can be obtained via the shift conditions. This means getting the values of $(b + c + e)$.

As a next step one needs to set the rest of $X_{(00)}^{(11)}$, for example the parameters b, c, d and f . This results in shift conditions of the form

$$X_{0,L,0,L}^{1,L,1,L} = X_{1,R,1,R}^{1,L,1,L}, \dots \tag{4.62}$$

These mean one will get the elements $\begin{smallmatrix} LL \\ RR' \end{smallmatrix}$ of the rest of the blocks, i.e. all of the parameters f are now known.

After that the rest of $X_{(10)}^{(11)}$ needs to be set, this means additionally fixing for example its b, c and d parameters. Shift conditions are now of the form

$$X_{1,L,0,L}^{1,L,1,L} = X_{1,L,1,R}^{1,L,1,L}, \dots \tag{4.63}$$

which means the knowledge of all of the $\begin{smallmatrix} LL \\ LR' \end{smallmatrix}$ elements, i.e. parameters b .

There are still some undetermined parameters, so the next step is again setting the rest of another block, for example the rest of $X_{(01)}^{(10)}$ and for example its parameters c and d . Shift conditions now will look like

$$X_{0,L,1,L}^{1,L,0,L} = X_{1,R,1,L}^{1,L,1,R}, \dots \tag{4.64}$$

meaning all of the $\begin{smallmatrix} LR \\ RL' \end{smallmatrix}$ elements can be obtained, which gives the values of $(a - d - f)$. This however means that in almost all of the first 16 blocks, except for the ones that have already been set completely during the process, is still one undetermined parameter. So there is a need to fix one more parameter from e.g. $X_{(10)}^{(00)}$. Let it be for example c , looking again at the shift conditions, which are of the form

$$X_{0,L,1,L}^{1,L,0,L} = X_{1,R,1,L}^{1,L,1,R}, \dots \tag{4.65}$$

it can be seen that all of the $\begin{smallmatrix} RR \\ LR' \end{smallmatrix}$ elements are determined now. This means only the values of $-c$ need to be additionally set.

Finally all of the 16 first blocks are now determined. During the process it was necessary to fix $6 + 5 + 4 + 3 + 2 + 1 = 21$ parameters which means that there can not be more that 21 attractors for the eigenvalue 1. However, 21 linearly independent attractors has already been constructed which means that the dimension of this eigenspace truly is 21.

4.6 Indistinguishable particles

Up until now this chapter has dealt with two distinguishable particles. The following section will now focus on the possibility of the two walkers being indistinguishable, i.e. bosonic or fermionic particles. As has been said in the previous chapter, the walkers now have to walk only in either the symmetrical (bosons) or antisymmetrical (fermions) subspace of the Hilbert space \mathcal{H} . With the evolution restricted only to these subspaces, it naturally follows that even the asymptotic states have to belong to them. For percolated quantum walks of indistinguishable particles the shift and coin conditions are naturally the same as for the distinguishable case. The only difference is that now the attractors also have to be only either symmetrical or antisymmetrical operators in the sense which will be explained in the next paragraphs. Quite straightforwardly the strategy is now to find the symmetrical and antisymmetrical subspaces of the already known attractor space for distinguishable walkers.

The projector on the bosonic symmetrical subspace $\mathcal{S}_2\mathcal{H}$ of the two-particle Hilbert space \mathcal{H} is given as

$$\mathcal{S}_2 = \frac{1}{2}(I + W), \quad (4.66)$$

where W is the operator defined in equation (4.41) and I is the two-particle identity. Clearly the operator \mathcal{S}_2 is Hermitian, so $\mathcal{S}_2 = \mathcal{S}_2^\dagger$. The (particle-wise) symmetrical part of the attractor $X \in \mathcal{B}(\mathcal{H})$ can be obtained via this projector as

$$X_S = \mathcal{S}_2 X \mathcal{S}_2^\dagger = \mathcal{S}_2 X \mathcal{S}_2. \quad (4.67)$$

Similarly for fermions the projector on the antisymmetrical subspace $\mathcal{A}_2\mathcal{H}$ is given as

$$\mathcal{A}_2 = \frac{1}{2}(I - W). \quad (4.68)$$

This projector is also hermitian and the (particle-wise) antisymmetrical part of the attractor X is then

$$X_A = \mathcal{A}_2 X \mathcal{A}_2. \quad (4.69)$$

As a small note it would now probably be useful to comment on why one can directly symmetrize, or antisymmetrize, the attractors. It is always important to point out the fact that attractors do not have to be possible density matrices on their own. Actually, as has been stated in the second chapter, if the attractor does not correspond to the eigenvalue $\lambda = 1$, then its trace is 0, so it will never be a valid density matrix. So when calculating basically any quality of the asymptotic evolution one should always construct the actual asymptotic state, using the initial density matrix of the system, first. It turns out that, from the properties of the formula for the asymptotic state, sometimes the qualities actually do transfer to attractors and one can work directly with them. This is truly the case for the bosonic and fermionic systems as will be now shown.

Since with the initial state in the correct symmetrical, or antisymmetrical, subspace the evolution stays in it, the asymptotic state will also be in the given subspace. Clearly for any general linear combination of operators

$$X = \sum_i c_i X_i, \quad \forall i, c_i \in \mathbb{C}, \quad (4.70)$$

it holds that

$$AXA^\dagger = \sum_i c_i AX_i A^\dagger, \quad (4.71)$$

for any operator A . So any asymptotic state will only be a linear combination of either symmetrical, or antisymmetrical attractors. The only question now are the coefficients of the linear combinations. These are originally given by the Hilbert-Schmidt scalar product of the initial state with the attractors.

In that case it is sufficient to show that even there only the symmetrical, or antisymmetrical attractors are relevant. Let ρ be a symmetrical density matrix, so that then $\rho = \mathcal{S}_2 \rho \mathcal{S}_2$. Based on this and the cyclic properties of the trace it then holds

$$\langle X, \rho \rangle_{HS} = \text{Tr} [X^\dagger \rho] = \text{Tr} [X^\dagger \mathcal{S}_2 \rho \mathcal{S}_2] = \text{Tr} [\mathcal{S}_2 X^\dagger \mathcal{S}_2 \rho] = \text{Tr} [(\mathcal{S}_2 X \mathcal{S}_2)^\dagger \rho] = \langle \mathcal{S}_2 X \mathcal{S}_2, \rho \rangle_{HS}. \quad (4.72)$$

The same can be shown for antisymmetrical ρ and \mathcal{A}_2 . So even with the coefficients one only needs to consider the symmetrized, or antisymmetrized attractors.

Taking a quick look at the common eigenstates $|\Phi_{++}\rangle$ and $|\Phi_{--}\rangle$, it is clear that both of them are symmetrical towards the swap of particles

$$\begin{aligned} \mathcal{S}_2 |\Phi_{++}\rangle &= |\Phi_{++}\rangle, & \mathcal{S}_2 |\Phi_{--}\rangle &= |\Phi_{--}\rangle, \\ \mathcal{A}_2 |\Phi_{++}\rangle &= 0, & \mathcal{A}_2 |\Phi_{--}\rangle &= 0. \end{aligned} \quad (4.73)$$

On the other hand a quick calculation reveals that

$$W |\Phi_{+-}\rangle = |\Phi_{-+}\rangle, \quad (4.74)$$

and in that case the symmetrized and antisymmetrized parts of these common eigenstates are

$$\begin{aligned} \mathcal{S}_2 |\Phi_{+-}\rangle &= \mathcal{S}_2 |\Phi_{-+}\rangle = \frac{1}{2} (|\Phi_{+-}\rangle + |\Phi_{-+}\rangle), \\ \mathcal{A}_2 |\Phi_{+-}\rangle &= -\mathcal{A}_2 |\Phi_{-+}\rangle = \frac{1}{2} (|\Phi_{+-}\rangle - |\Phi_{-+}\rangle). \end{aligned} \quad (4.75)$$

As for the non-separable common eigenstate $|\Phi_w\rangle$, it is again symmetrical, so

$$\mathcal{S}_2 |\Phi_w\rangle = |\Phi_w\rangle, \quad \mathcal{A}_2 |\Phi_w\rangle = 0. \quad (4.76)$$

All in all, for bosons there are only 4 different common eigenstates left after symmetrization ($|\Phi_{++}\rangle$, $|\Phi_{--}\rangle$, $\mathcal{S}_2 |\Phi_{+-}\rangle$, $|\Phi_w\rangle$), so the subspace of p-attractors is now only 16-dimensional while originally it was 25. For fermions there is only one antisymmetric common eigenstate left, and that is $\mathcal{S}_2 |\Phi_{+-}\rangle = \frac{1}{2} (|\Phi_{+-}\rangle + |\Phi_{-+}\rangle)$. So for fermionic walkers only one p-attractor survived the antisymmetrization.

Moving on to the non-p-attractors, lets first take a look at the attractors constructed from one-particle identity $I^{(1)}$ and a general one-particle p-attractor $|v_1 \chi v_2\rangle$ via the tensor product. Clearly it holds that

$$\begin{aligned} \mathcal{S}_2 (I^{(1)} \otimes |v_1 \chi v_2\rangle) \mathcal{S}_2 &= \frac{1}{4} [I^{(1)} \otimes |v_1 \chi v_2\rangle + \\ &+ |v_1 \chi v_2\rangle \otimes I^{(1)} + W (I^{(1)} \otimes |v_1 \chi v_2\rangle) + (I^{(1)} \otimes |v_1 \chi v_2\rangle) W]. \end{aligned} \quad (4.77)$$

Quick computation also reveals that in fact

$$\begin{aligned} W (I^{(1)} \otimes |v_1 \chi v_2\rangle) &= (|v_1 \chi v_2\rangle \otimes I^{(1)}) W, \\ (I^{(1)} \otimes |v_1 \chi v_2\rangle) W &= W (|v_1 \chi v_2\rangle \otimes I^{(1)}), \end{aligned} \quad (4.78)$$

and because of that

$$\mathcal{S}_2 (I^{(1)} \otimes |v_1 \chi v_2\rangle) \mathcal{S}_2 = \mathcal{S}_2 (|v_1 \chi v_2\rangle \otimes I^{(1)}) \mathcal{S}_2. \quad (4.79)$$

So the 8 non-p-attractors constructed this way will reduce to 4 symmetrized ones and the identity will become $\mathcal{S}_2 = \frac{1}{2} (I + W)$. As for the rest of the non-p-attractors constructed using the W operator, it also holds that

$$\mathcal{S}_2 W X \mathcal{S}_2 = \frac{1}{4} (W X + X + W X W + X W) = \mathcal{S}_2 X \mathcal{S}_2. \quad (4.80)$$

From that it is obvious that they do not give us any additional symmetrized attractors, so one is left with 5 non-p-attractors for bosonic walkers.

For fermionic case it can be very similarly shown that

$$\begin{aligned} \mathcal{A}_2 \left(I^{(1)} \otimes |v\chi v\rangle \right) \mathcal{A}_2 &= \frac{1}{4} [I^{(1)} \otimes |v\chi v\rangle + \\ &+ |v\chi v\rangle \otimes I^{(1)} - W \left(I^{(1)} \otimes |v\chi v\rangle \right) - \left(I^{(1)} \otimes |v\chi v\rangle \right) W], \end{aligned} \quad (4.81)$$

and also

$$\mathcal{A}_2 W X \mathcal{A}_2 = \frac{1}{4} (W X - X - W X W + X W) = -\mathcal{A}_2 X \mathcal{A}_2. \quad (4.82)$$

So clearly all of the non-p-attractors except for the identity will reduce to 4 antisymmetrized non-p-attractors and the identity will become $\mathcal{A}_2 = \frac{1}{2} (I - W)$.

All together this yields $16 + 5 = 21$ attractors for bosons and $1 + 5 = 6$ attractors for fermions for the finite lines and circles of lengths $N \neq 4k, \forall k \in \mathbb{N}$. For the circles of lengths $N = 4k, \forall k \in \mathbb{N}$ there will only be \mathcal{A}_2 for fermions and $|\Phi_w\rangle\langle\Phi_w|$ together with \mathcal{S}_2 for bosons.

4.7 Asymptotic state for circles of lengths $N \neq 4k$

As promised earlier in this chapter, the case of circles of lengths $N \neq 4k$ will now be analyzed more in detail, since in this case the number of attractors reduces greatly. Another thing which makes this special case much simpler is the fact, that there is only one eigenvalue present and that is 1. So the resulting asymptotic state will be stationary as can be seen from the general formula (2.19). First necessary thing to do is to get the orthogonal basis. For circles of length $N \neq 4k$ one is left with only three attractors normalized to unit trace. These are the normalized global identity $\frac{1}{2N}I$, normalized SWAP operator

$$\tilde{W} \equiv \frac{1}{2N} W = \frac{1}{2N} \sum_{x,y=0}^{N-1} \sum_{i,j=\{L,R\}} |x, i, y, j\rangle \langle y, j, x, i|, \quad (4.83)$$

and the projector onto the common eigenstate $|\Phi_w\rangle$

$$F \equiv |\Phi_w\rangle \langle\Phi_w|. \quad (4.84)$$

Considering that $|\Phi_w\rangle$ can be re-written in the form

$$|\Phi_w\rangle = \frac{1}{\sqrt{2N}} \sum_{x=0}^{N-1} \sum_{i=\{L,R\}} |x, i, x, i\rangle, \quad (4.85)$$

the F operator can actually be written as

$$F = \frac{1}{2N} \sum_{x,y=0}^{N-1} \sum_{i,j=\{L,R\}} |x, i, x, i\rangle \langle y, j, y, j|. \quad (4.86)$$

By performing the Gram-Schmidt orthogonalization on the three attractors above it is possible to obtain the following basis

$$\begin{aligned} A_1 &= \frac{1}{2N} I, \\ A_2 &= \frac{2N}{\sqrt{4N^2 - 1}} \left(\tilde{W} - \frac{1}{2N} A_1 \right), \\ A_3 &= \sqrt{\frac{N(2N+1)}{(N+1)(2N-1)}} \left(F - \frac{1}{2N} A_1 - \frac{1}{2N} \sqrt{\frac{2N-1}{2N+1}} A_2 \right). \end{aligned} \quad (4.87)$$

It is now necessary to choose a specific initial state and make the projection onto the attractor space. Let us first consider the initial state of the two particles localized at 0 vertex with an arbitrary pure coin state

$$|\psi_0\rangle = |0, 0\rangle \otimes (a|LL\rangle + b|LR\rangle + c|RL\rangle + d|RR\rangle), \quad (4.88)$$

where the coefficients $a, b, c, d \in \mathbb{C}$ satisfy the normalization condition

$$|a|^2 + |b|^2 + |c|^2 + |d|^2 = 1. \quad (4.89)$$

Evaluating the Hilbert-Schmidt scalar products of the initial density matrix and the orthonormalized attractors A_j one finds the asymptotic state of the two-particle percolated walk of the form

$$\rho_\infty = \frac{1}{2N}A_1 + \frac{2N-1-2N|b-c|^2}{2N\sqrt{4N^2-1}}A_2 + \frac{(2N+1)|a+d|^2+|b-c|^2-2}{2\sqrt{N(N+1)(4N^2-1)}}A_3. \quad (4.90)$$

For further analysis it is usually more suitable to express the asymptotic state in terms of the identity I , normalized SWAP operator \tilde{W} and the projector onto $|\Phi_w\rangle$. By doing that one finds the following

$$\rho_\infty = \frac{2N+|b-c|^2-|a+d|^2}{4N(2N^2+N-1)}I - \frac{|a+d|^2+(2N+1)|b-c|^2-2N}{2(2N^2+N-1)}\tilde{W} + \frac{(2N+1)|a+d|^2+|b-c|^2-2}{2(2N^2+N-1)}F. \quad (4.91)$$

It can be shown that the same asymptotic state can be obtained even for non-localized initial state of for initial states localized at different vertex than 0. More specifically one can extend the initial positions of the walkers to the equal superposition of all states where they are at the same vertex (diagonal terms). Even the equal superposition of all possible positions of the two walkers yields the same resulting asymptotic state if one keeps the local coin state identical for all positions.

Another example can be initial state where the walkers start at arbitrary, but different positions x and y . The initial state will then be

$$|\psi_0\rangle = |x, y\rangle \otimes (a|LL\rangle + b|LR\rangle + c|RL\rangle + d|RR\rangle), \quad x \neq y, \quad (4.92)$$

where the coefficients $a, b, c, d \in \mathbb{C}$ again satisfy the normalization condition (4.89). This case is interesting because the resulting asymptotic state does not depend on the choice of the initial coin state at all. The asymptotic state will always be equal to

$$\rho_\infty = \frac{1}{2N}A_1 - \frac{1}{2N\sqrt{4N^2-1}}A_2 - \frac{1}{2N}\sqrt{\frac{N}{(N+1)(4N^2-1)}}A_3, \quad (4.93)$$

which rewritten into I, \tilde{W} and F gives the formula

$$\rho_\infty = \frac{2N+1}{4N(2N^2+N-1)}I - \frac{1}{2(2N^2+N-1)}\tilde{W} - \frac{1}{2(2N^2+N-1)}F. \quad (4.94)$$

There are again more initial states which will result in this asymptotic behavior. These are for example all pure initial states where the coin state is again the same for all positions and position-wise the walkers have zero probability of being on the same vertex.

4.8 Mapping to one-particle walk

This small section concerns itself with the question, whenever or not it is possible to somehow usefully map the two-particle quantum walk in one dimension to one-particle quantum walk in two dimensions. It may be tempting to try to use the results of one-particle walk on a 2D lattice in some way, because at least the dimensions of the corresponding Hilbert spaces are the same. Here it will be pointed out why it is not so straightforward and why the results for percolated walk on a 2D lattice [28] are completely different from the ones obtained in earlier sections of this work.

The most natural idea, how to do the mapping, is to take the positions of the two particles on a line x, y and make them a position of one particle on a 2D lattice (x, y) . The question now is, how does the new shift operator look like, i.e. what do the coin states map to. Looking at a walk which is not lazy and non-percolated, clearly in every step both indices (positions of the original two particles) have to change ± 1 . This means it is not possible to make the following moves in one step of the walk

$$(x, y) \rightarrow (x \pm 1, y), \quad (x, y) \rightarrow (x, y \pm 1). \quad (4.95)$$

So it is not possible to go to the neighboring vertices on the 2D lattice at all. In fact, there will be 2 disjoint half sized 2D lattices on which the particle will walk. One of the lattices will start at $(0, 0)$ and the other at $(0, 1)$. So the evolution of non-percolated and not lazy walk of two particles on a line can be mapped to one-particle walk on 2 disjoint half sized 2D lattices. Since the evolution on those lattices is also disjoint, it can be put together by evolving the corresponding parts of the initial state separately as normal walks on a lattice.

Lazy walk would of course allow jumping even to the neighboring vertices alongside the original ones. This basically represents 'gluing' the two lattices together by additional edges. Much more interesting is to observe, what exactly will the percolations do. By writing down all the possible configurations on the positions of the two particles, one can witness the edges reconnecting. Except for the cases when none of the edges $(x, x + 1), (x - 1, x), (y, y + 1), (y - 1, y)$ exist (the corresponding edges will then truly disappear) the edges in the two lattices will just reconnect in some way to create a link between the two. The underlying graph is the one from the lazy walk, but some edges clearly can not exist together, i.e. only some percolations are allowed. Clearly the graph is not only no longer a simple 2D lattice(s), but also the percolations are not arbitrary.

Even though this mapping is nor very straightforward nor does seem very useful, it provides an interesting insight, and more importantly visualization, about how does percolation work for more walkers. There are of course many other possible mappings. However even this one already shows that one can possibly get dynamics of one walker on much more complex systems simply by adding more walkers on a simple but percolated graphs.

4.9 Possible extensions

The last short note of this work will be concerned with some thoughts on possible extensions of the studied model. The first thing that can be considered is the generalization of the local coin operator used. As has been shown at the beginning of this work in Section 1.2, there are many coins for which the resulting evolutions are equivalent. That is a reason to believe that for great number of local coins the results of two-walker percolated quantum walks in one dimension will be very similar to the ones obtained for the Hadamard coin. However, the situation will surely become more complicated for the class of coins for which the one-particle case has more non-p-attractors than just the identity which has been mentioned in [27]. There, as one can see from the earlier construction of two-particle attractors,

will have to be much more attractors than for the case analyzed here. So in this direction one would expect the situation to become even more difficult to analyze.

Another direction of thought can be the three-state quantum walk in one dimension, i.e. the lazy walk. As has been shown earlier, for the single-walker case the lazy walk can for some coins demonstrate the positive effect of percolations on the transport properties of the system. More specifically it can be showed that percolations have a tendency to destroy the localized eigenvalues of the original non-percolated unitary evolution. From the tensor structure of the problem it is clear that this effect would also be present for the two-particle walk at least for the same class of coins. As for the transport properties of the two-state walk it is maybe worth noting that all of the found attractors are spanned across the whole graph, so there are no localized attractors. However, as the non-percolated evolution also does not show any localizations, it is not much of a surprise.

Finally, adding interaction to the problem is probably the most attractive possible direction of the future work. As has also been shown by some of the numerical results from [40], the interplay between the interaction and percolations would definitely be interesting to study. However, in this case one can obviously no longer rely on the one-particle results which made the non-interaction case easier to analyze.

Conclusion

In summary, this work studied the two-walker discrete-time quantum walks in one dimension, specifically the asymptotic evolution of the dynamically percolated non-interacting model with the Hadamard coin. In the beginning, the first chapter introduced the discrete-time quantum walks in general and later focused in more detail on the special case of the walk on a line and its solutions. The second chapter then discussed quantum walks on dynamically percolated graphs, i.e. graphs whose edges can randomly break and reappear during the time evolution. It introduced the formalism used to study the time evolution of such systems in the asymptotic limit of large number of steps of the walk. It then also presented the known results for single-walker percolated walks on a finite line and a circle. The focus of the third chapter was on the two-particle quantum walks in one dimension. Some of the previous works on this topic were reviewed in this chapter first for the simple non-interacting case and later also for the possible interaction between the walkers. At last this chapter also reviewed the two previous works concerning the percolated two-walker walks. These works are numerical studies of the model discussed in the last chapter with [40] and without interaction [39] present. The last chapter then finally discussed the obtained results for the non-interacting two-walker discrete-time quantum walks in one dimension with dynamical percolations.

By allowing dynamical percolations, i.e. random breaking of edges, the asymptotic evolution of the system can be found analytically. More specifically it is possible to find a subspace of the bounded operators on the systems' Hilbert space, the attractor subspace, in which the density matrix of the system stays in the asymptotic limit. So by finding the orthonormal basis of attractors of such system, one can then project the initial density matrix of the system onto this attractor space to study the asymptotic evolution. The resulting evolution is then usually quasi-periodic depending on the corresponding eigenvalues.

As for the obtained results, it was proved that the attractor space is 43-dimensional for all finite lines and for circles of lengths $N = 4k, \forall k \in \mathbb{N}$. For other circles the dimension quite drastically reduces to 3 because of the periodic boundary conditions. As for the eigenvalues to which these attractors correspond, there are four of them - 1, -1, i and $-i$. The corresponding normalized and linearly independent set of attractors was found as well, however, they are not orthogonal and hence do not form an orthonormal basis. Due to the great number of attractors the orthonormalization was done only for the case of circles of lengths $N \neq 4k, \forall k \in \mathbb{N}$, where there are only 3 attractors present. The case of indistinguishable walkers was then also discussed. It turns out it is possible to obtain the attractors for the bosonic and fermionic cases simply by projecting the found attractors onto the particle-wise symmetrical and antisymmetrical subspaces. This actually reduces the number of attractors for both types of indistinguishable particles, for the case of fermionic walkers this reduction is quite significant. An interesting thing to notice is that while it is possible to construct a large part of the attractor space from the one-particle asymptotic evolution, there are also purely two-particle terms.

Finally, the work also showed an example solution to finding the actual asymptotic state for the case of the circle of length $N \neq 4k, \forall k \in \mathbb{N}$, for several examples of initial states of the system. At last it briefly commented on the possible future work regarding the topic.

Bibliography

- [1] Y. Aharonov, L. Davidovich, and N. Zagury, “Quantum random walks,” *Physical Review A*, vol. 48, Aug 1993.
- [2] S. Chakraborty, L. Novo, A. Ambainis, and Y. Omar, “Spatial search by quantum walk is optimal for almost all graphs,” *Physical Review Letters*, vol. 116, Mar 2016.
- [3] A. M. Childs, “Universal computation by quantum walk,” *Phys. Rev. Lett.*, vol. 102, p. 180501, May 2009.
- [4] A. M. Childs, D. Gosset, and Z. Webb, “Universal computation by multiparticle quantum walk,” *Science*, vol. 339, pp. 791–794, Feb 2013.
- [5] N. B. Lovett, S. Cooper, M. Everitt, M. Trevers, and V. Kendon, “Universal quantum computation using the discrete-time quantum walk,” *Phys. Rev. A*, vol. 81, p. 042330, Apr 2010.
- [6] S. Singh, P. Chawla, A. Sarkar, and C. M. Chandrashekar, “Universal quantum computing using single-particle discrete-time quantum walk,” *Scientific Reports*, vol. 11, Jun 2021.
- [7] J. Mareš, J. Novotný, and I. Jex, “Percolated quantum walks with a general shift operator: From trapping to transport,” *Physical Review A*, vol. 99, Apr 2019.
- [8] J. Mareš, J. Novotný, M. Štefaňák, and I. Jex, “Counterintuitive role of geometry in transport by quantum walks,” *Physical Review A*, vol. 101, Mar 2020.
- [9] J. Mareš, J. Novotný, and I. Jex, “Quantum walk transport on carbon nanotube structures,” *Physics Letters A*, vol. 384, May 2020.
- [10] J. Novotný, G. Alber, and I. Jex, “Asymptotic evolution of random unitary operations,” *Open Physics*, vol. 8, Jan 2010.
- [11] A. M. Childs, “On the relationship between continuous- and discrete-time quantum walk,” *Communications in Mathematical Physics*, vol. 294, Oct 2009.
- [12] M. Maniġhalaṃ and M. Kon, “General methods and properties to evaluate continuum limits of the 1d discrete time quantum walk,” *Quantum Information Processing*, vol. 19, Oct 2020.
- [13] F. W. Strauch, “Connecting the discrete- and continuous-time quantum walks,” *Physical Review A*, vol. 74, Sep 2006.
- [14] M. N. Dheeraj and T. A. Brun, “Continuous limit of discrete quantum walks,” *Physical Review A*, vol. 91, Jun 2015.

- [15] A. Ambainis, J. Kempe, and A. Rivosh, “Coins make quantum walks faster,” *Proceedings of the Annual ACM-SIAM Symposium on Discrete Algorithms*, Mar 2004.
- [16] S. K. Goyal, T. Konrad, and L. Diósi, “Unitary equivalence of quantum walks,” *Physics Letters A*, vol. 379, Jan 2015.
- [17] E. Bach, S. Coppersmith, M. P. Goldschen, R. Joynt, and J. Watrous, “One-dimensional quantum walks with absorbing boundaries,” *Journal of Computer and System Sciences*, vol. 69, Jul 2004.
- [18] T. G. Wong, “Grover search with lackadaisical quantum walks,” *Journal of Physics A: Mathematical and Theoretical*, vol. 48, Oct 2015.
- [19] T. G. Wong, “Faster search by lackadaisical quantum walk,” *Quantum Information Processing*, vol. 17, Feb 2018.
- [20] M. L. Rhodes and T. G. Wong, “Search by lackadaisical quantum walks with nonhomogeneous weights,” *Physical Review A*, vol. 100, Oct 2019.
- [21] M. L. Rhodes and T. G. Wong, “Search on vertex-transitive graphs by lackadaisical quantum walk,” *Quantum Information Processing*, vol. 19, Sep 2020.
- [22] L. K. Grover, “A fast quantum mechanical algorithm for database search,” in *Proceedings of the Twenty-Eighth Annual ACM Symposium on Theory of Computing*, STOC '96, (New York, NY, USA), Association for Computing Machinery, 1996.
- [23] A. Nayak and A. Vishwanath, “Quantum walk on the line,” arXiv: <https://arxiv.org/abs/quant-ph/0010117>, 2000.
- [24] B. Tregenna, W. Flanagan, R. Maile, and V. Kendon, “Controlling discrete quantum walks: coins and initial states,” *New Journal of Physics*, vol. 5, Jul 2003.
- [25] A. Kempf and R. Portugal, “Group velocity of discrete-time quantum walks,” *Physical Review A*, vol. 79, May 2009.
- [26] J. Novotný, G. Alber, and I. Jex, “Random unitary dynamics of quantum networks,” *Journal of Physics A: Mathematical and Theoretical*, vol. 42, Jun 2009.
- [27] B. Kollár, J. Novotný, T. Kiss, and I. Jex, “Discrete time quantum walks on percolation graphs,” *The European Physical Journal Plus*, vol. 129, May 2014.
- [28] B. Kollár, J. Novotný, T. Kiss, and I. Jex, “Percolation induced effects in two-dimensional coined quantum walks: analytic asymptotic solutions,” *New Journal of Physics*, vol. 16, Feb 2014.
- [29] J. Mareš, J. Novotný, M. Štefaňák, and I. Jex, “Key graph properties affecting transport efficiency of flip-flop grover percolated quantum walks,” *Physical Review A*, vol. 105, Jun 2022.
- [30] M. Štefaňák, J. Novotný, and I. Jex, “Percolation assisted excitation transport in discrete-time quantum walks,” *New Journal of Physics*, vol. 18, Feb 2016.
- [31] M. Štefaňák, I. Bezděková, and I. Jex, “Continuous deformations of the grover walk preserving localization,” *The European Physical Journal D*, vol. 66, May 2012.
- [32] M. Štefaňák, I. Bezděková, I. Jex, and S. M. Barnett, “Stability of point spectrum for three-state quantum walks on a line,” *Quantum Information and Computation*, vol. 14, Oct 2014.

- [33] Y. Omar, N. Paunković, L. Sheridan, and S. Bose, “Quantum walk on a line with two entangled particles,” *Phys. Rev. A*, vol. 74, Oct 2006.
- [34] M. Štefaňák, T. Kiss, I. Jex, and B. Mohring, “The meeting problem in the quantum random walk,” *Journal of Physics A: Mathematical and General*, vol. 39, Nov 2006.
- [35] M. Štefaňák, S. M. Barnett, B. Kollár, T. Kiss, and I. Jex, “Directional correlations in quantum walks with two particles,” *New Journal of Physics*, vol. 13, Mar 2011.
- [36] D. Li, J. Zhang, F. Guo, W. Huang, Q. Wen, and H. Chen, “Discrete-time interacting quantum walks and quantum hash schemes,” *Quantum Information Processing*, vol. 12, 03 2013.
- [37] S. D. Berry and J. B. Wang, “Two-particle quantum walks: Entanglement and graph isomorphism testing,” *Phys. Rev. A*, vol. 83, Apr 2011.
- [38] A. Ahlbrecht, A. Alberti, D. Meschede, V. B. Scholz, A. H. Werner, and R. F. Werner, “Molecular binding in interacting quantum walks,” *New Journal of Physics*, vol. 14, p. 073050, Jul 2012.
- [39] L. Rigovacca and C. D. Franco, “Two-walker discrete-time quantum walks on the line with percolation,” *Scientific Reports*, vol. 6, Feb 2016.
- [40] X. Sun, Q. Wang, and Z. Li, “Interacting two-particle discrete-time quantum walk with percolation,” *International Journal of Theoretical Physics*, vol. 57, Aug 2018.
- [41] R. F. Werner, “Quantum states with einstein-podolsky-rosen correlations admitting a hidden-variable model,” *Phys. Rev. A*, vol. 40, Oct 1989.